IMPROVED METHODS FOR PHASE DENSITY PREDICTION: CO_2 + HYDROCARBONS

By

MAHMUD SUDIBANDRIYO

Bachelor of Engineering

Bandung Institute of Technology

Bandung, Indonesia

1986

Submitted to the Faculty of the
Graduate College of the
Oklahoma State University
in partial fulfillment of
the requirements for
the Degree of
MASTER OF SCIENCE
May, 1991

IMPROVED METHODS FOR PHASE DENSITY

PREDICTION: CO_2 + HYDROCARBONS

Thesis Approved:

K.A.M. Gasem
Thesis Adviser

Jan Wagner

Arlund H. Johannes

Norman N. Durham
Dean of the Graduate College

PREFACE

Improved methods for mixture phase density predictions were developed. First, scaling-law theory was introduced in the volume translation concept which results in simpler form and better representation for saturation densities of CO_2-hydrocarbon mixtures than that given by Peneloux's volume translation. Second, the scaled-variable-reduced-coordinate (SVRC) method was extended to the prediction of mixture densities.

Using the extended SVRC correlation, mixture density predictions may be performed based on pure-fluid properties, or more precisely based on some mixture data. Both treatments gave comparable results with the existing methods in the literature with the added advantage of covering the full saturation range and obeying scaling-law behavior in the near-critical region. Generalized SVRC correlations provide adequate liquid and vapor density predictions (2 and 7 % AAD, respectively). The quality of these predictions, however, is enhanced by the flexibility offered by one system-specific parameter.

I wish to express my gratitude to all the people who assisted me during my stay at Oklahoma State University. In particular, I sincerely thank Dr. K. A. M. Gasem, my major advisor, for his guidance, knowledge and understanding,

which were of tremendous help to me. I would like to thank my advisor for allowing me the chance to pursue this study and for his unforgettable warmth and generosity.

I am also grateful to the other committee members, Dr. A. J. Johannes and Dr. Jan Wagner, for their advisement and valuable input.

TABLE OF CONTENTS

LIST OF TABLES

LIST OF FIGURES

Figure Page

NOMENCLATURE

Symbols

A,B a,b	cubic equation of state parameters
A,B,C	correlation constants used in SVRC
A_1,A_2 a_1,a_2	parameters in cubic EOS with volume translation
a	Helmholtz energy
c	translation constant
C_{ij} ,D_{ij}	binary interaction parameters in cubic EOS
D	dimensionless distance variable
d	distance variable
D,E,F	coefficient in the reduced form of cubic EOS
f	molecular conformal volume parameter
h	molecular conformal energy parameter
K	equilibrium constant
k	Boltzmann's constant
L	total moles of liquid
N	total number of moles
P	vapor pressure
R	gas constant
RMSE	root mean square error
T	temperature
t	translation constant

u,w	constants in generalized form of cubic EOS
V	specific volume
x,y,z	composition
X	independent correlating variable
Y	saturated fluid property
Z	compressibility factor
ZRA	Rackett's compressibility factor
% AAD	average absolute percent deviation

Greek

$\alpha,\beta,\delta,\gamma$	parameters in Martin's equation of state
α,β,Δ	universal constants in scaling-law behavior
β	compressibility
δ	volume shift
Δ	change in property
$\Delta\alpha$	$\alpha_c - \alpha_i$
ε	energy parameter of molecular interaction; reduced variable
ϵ	convergence tolerance
ϕ	fugacity coefficient; saturation property
η	universal constant used in Prausnitz's volume translation
θ	correlating function in SVRC; surface fraction
ρ	density
σ	saturation condition
υ	parameter in equation (27)

Superscript

C	classical
D	deviation
id	ideal
L	liquid
m	model
NC	nonclassical
r	residual
SRK-VT	Soave-Redlich-Kwong volume translation
V	vapor

Subscript

c	critical point state
calc	calculated
exp	experimental
i	initial; component i
j	component j
m,M	maximum; mixture
r	reduced property
SRK	Soave-Redlich-Kwong
t	triple point state or the lowest value of the properties

CHAPTER I

INTRODUCTION

Thermodynamic properties play a major role in both the theoretical understanding of fluid phase behavior and in the practice of chemical engineering. This is evident from the fact that most of the investment and the energy related operating costs in a typical chemical plant involve separation and purification equipment, which are designed largely on the basis of phase equilibrium properties.

Because of their importance in process design, many thermodynamic and physical property models have been developed. The majority of existing models are analytic equations of state or correlations based on corresponding states theory.

Cubic equations of state are highly efficient in correlating thermodynamic properties. In general, however, they are incapable of accurately predicting phase densities, especially near the critical point. While the volume translation concept, which was introduced by Martin [20] and further illustrated by Peneloux [25], does improve the density predictions far from the critical, it fails to do so near the critical point. In 1988 Chou and Prausnitz corrected this deficiency; however, their model is difficult

to apply for mixtures.

The CST methods have been more successful in predicting phase densities. Several investigators have proposed the calculation of saturated liquid molar volume based on the corresponding states theory [16,30,31,40]. In 1979 Hankinson and Thomson [16] presented their correlation for the prediction of saturated molar volume which gave better results compared to the Yen-Woods correlation [40] and the Rackett equation as modified by Spencer and Danner [31].

Recently, Gasem and co workers [30] have proposed the scaled-variable-reduced-coordinate (SVRC) model which utilizes the CST concepts. The SVRC model has been proven capable of accurately representing a number of saturation properties of pure fluids over the full saturation range from the triple point to the critical point.

The objective of this study was to develop a model capable of accurately predicting a number of liquid and vapor phase properties of mixtures over the entire saturation region. More specifically, work was directed at the prediction of saturated density of CO_2 + hydrocarbon binary mixtures over a pressure range up to the critical point of the mixtures.

Two approaches have been pursued in this study to achieve the stated objective; the EOS approach and the SVRC approach. The EOS approach involved the following tasks:

(1) evaluation of the functional behavior of van der Waals

type cubic equations of state (Redlich-Kwong, Soave-Redlich-Kwong, and Peng-Robinson equations),

(2) development of an effective strategy for solving cubic equations of state,

(3) evaluation of the existing volume translation methods for saturated density predictions, and

(4) development of new model for volume translation.

The SVRC approach involved:

(1) evaluation of the existing mixing rules,

(2) development of appropriate mixing rules for the SVRC method, and

(3) development of a generalized SVRC model for the CO_2 + hydrocarbon mixtures.

Liquid and vapor phase density measurements acquired at Oklahoma State University [see, e.g., 13] for CO_2 + hydrocarbon binaries have been used in our evaluations.

CHAPTER II

GENERALIZED CUBIC EQUATION OF STATE

An equation of state is an analytical expression relating pressure, volume, temperature, and composition of a given system. The importance and necessity of accurate equations of state are reflected by the appearance of numerous such equations in the literature. The development of these equations started from the ideal gas law expression to modern-day equations of state.

In industrial application, especially in hydrocarbon processing, the evolution paths for equations of state have been noted by Edmister [10] to be:

Path 1. van der Waals ----> Redlich-Kwong ----> Wilson ----> Soave and Peng-Robinson.

Path 2. Beattie-Bridgeman ----> Benedict-Webb-Rubin ----> Starling ----> Starling-Han.

Path 3. Thiele ----> Carnahan-Starling ----> Beret-Prausnitz ----> Donahue-Prausnitz.

The development of the first two paths was essentially empirical and the development of the last one was theoretical. The equations of state listed in the first path are most widely used in hydrocarbon processing

because of their simplicity. These equations are given in cubic form and have only two adjustable parameters. Furthermore, these simple forms have an accuracy that compares quite favorably with the more complex equations of state. Therefore, in the present work, we will be concerned only with cubic equations of state.

A generic expression for the currently popular cubic equations of state may be presented in this general form:

$$P = \frac{RT}{V-b} - \frac{a}{V^2 + ubV + wb^2} \qquad (1)$$

Definitions for a, b, u, and w are specific for the equation of state used. Features of some specific cubic equations of state are listed in Table I.

TABLE I

FEATURES OF SOME SPECIFIC CUBIC EQUATIONS OF STATE

EOS	u	w	a	b	α
VDW	0	0	$(27/64)(RTc)^2/Pc$	$RTc/8Pc$	-
RK	1	0	$0.42748\alpha(RTc)^2/Pc$	$0.08664RTc/Pc$	$Tr^{-0.5}$
SRK	1	0	$0.42748\alpha(RTc)^2/Pc$	$0.08664RTc/Pc$	$[1+(0.48+1.574\omega -0.176\omega^2)(1-Tr^{0.5})]^2$
PR	2	-1	$0.457235\alpha(RTc)^2/Pc$	$0.077796RTc/Pc$	$[1+(0.37646+1.54226 -0.26992\omega^2)(1-Tr^{0.5})]^2$

Solution of Generalized Cubic Equation of State

A first requirement for applying any equation of state to the calculation of thermodynamic properties is to solve the desired equation for the molar volume (V) or the compressibility factor (Z) at given temperature, pressure and composition. Equation (1) may be rearranged into the reduced cubic equation of state form

$$F(Z) \equiv Z^3 + D\,Z^2 + E\,Z - F = 0 \qquad (2)$$

The coefficients for this equation are given as:

$$D = uB - B - 1 \qquad (3)$$

$$E = wB^2 - uB^2 - uB + A \qquad (4)$$

$$F = wB^3 + wB^2 + BA \qquad (5)$$

Values of u and w are listed in Table I, and A and B are reduced equation of state parameters defined as:

$$A = aP/(RT)^2 \qquad (6)$$

$$B = bP/RT \qquad (7)$$

where b is an empirical constant and a is a function of temperature. Definitions for a and b for some equations of state are listed in Table I.

Before discussing methods for finding Z, it is important to examine the functional behavior of Equation (2).

Functional Behavior of F(Z) with Z

Examination of the functional behavior of F(Z) with Z has been addressed by several investigators [4,10,15,17]. Most have analyzed this behavior mathematically. Figure 1 shows the typical functional behavior of P(V) with V which can be related to the functional behavior of F(Z) with Z (Figure 2). These figures appeared in the article written by Gosset [15]. Similarly, Jovanovic [17] presented the possible forms of F(Z) as shown in Figure 3.

In this study, the possible forms of F(Z) are evaluated by plotting F(Z) with respect to Z for a given pressure and temperature, and by evaluating inflection points of F(Z) for specific values of the equation of state constants A and B. To generate F(Z) plots, the equation of state constants A and B are calculated utilizing Equations (6) and (7) and the parameter definitions given in Table I. The coefficients of Equation (2) are then calculated and F(Z) is determined for a given value of Z. Values of Z are selected between zero and three, since only positive values of Z are meaningful and, in most cases, the value of Z will not exceed three.

Figures 4-6 show the plot of F(Z) with respect to Z for pure CO_2. Temperature is chosen in the supercritical region, at the critical point, in the subcritical region, and at the triple point or close to the triple point. A similar three dimensional plot is shown in Figure 7.

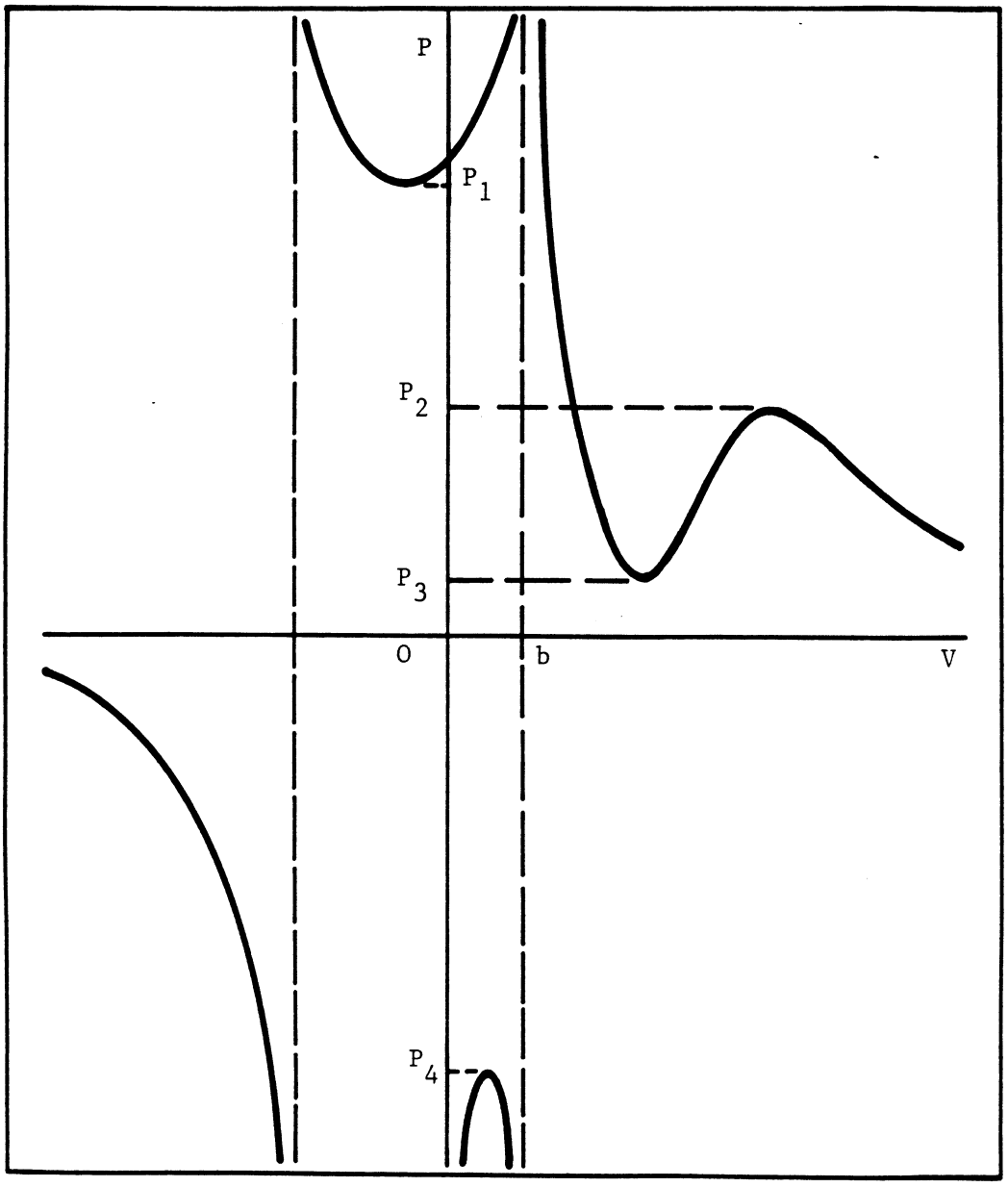

Figure 1. P(V) Functional Behavior

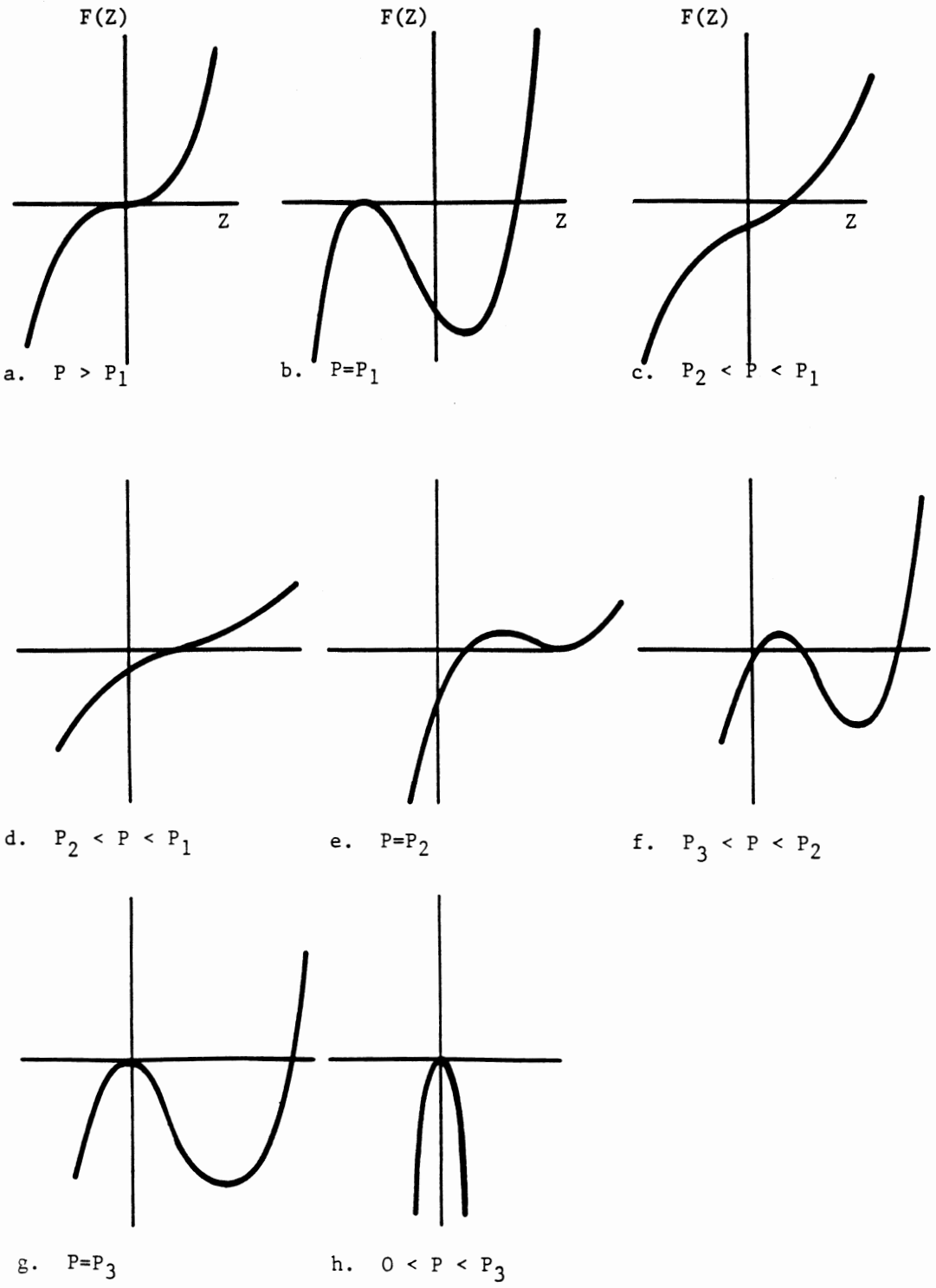

Figure 2. F(Z) Functional Behavior (Gosset)

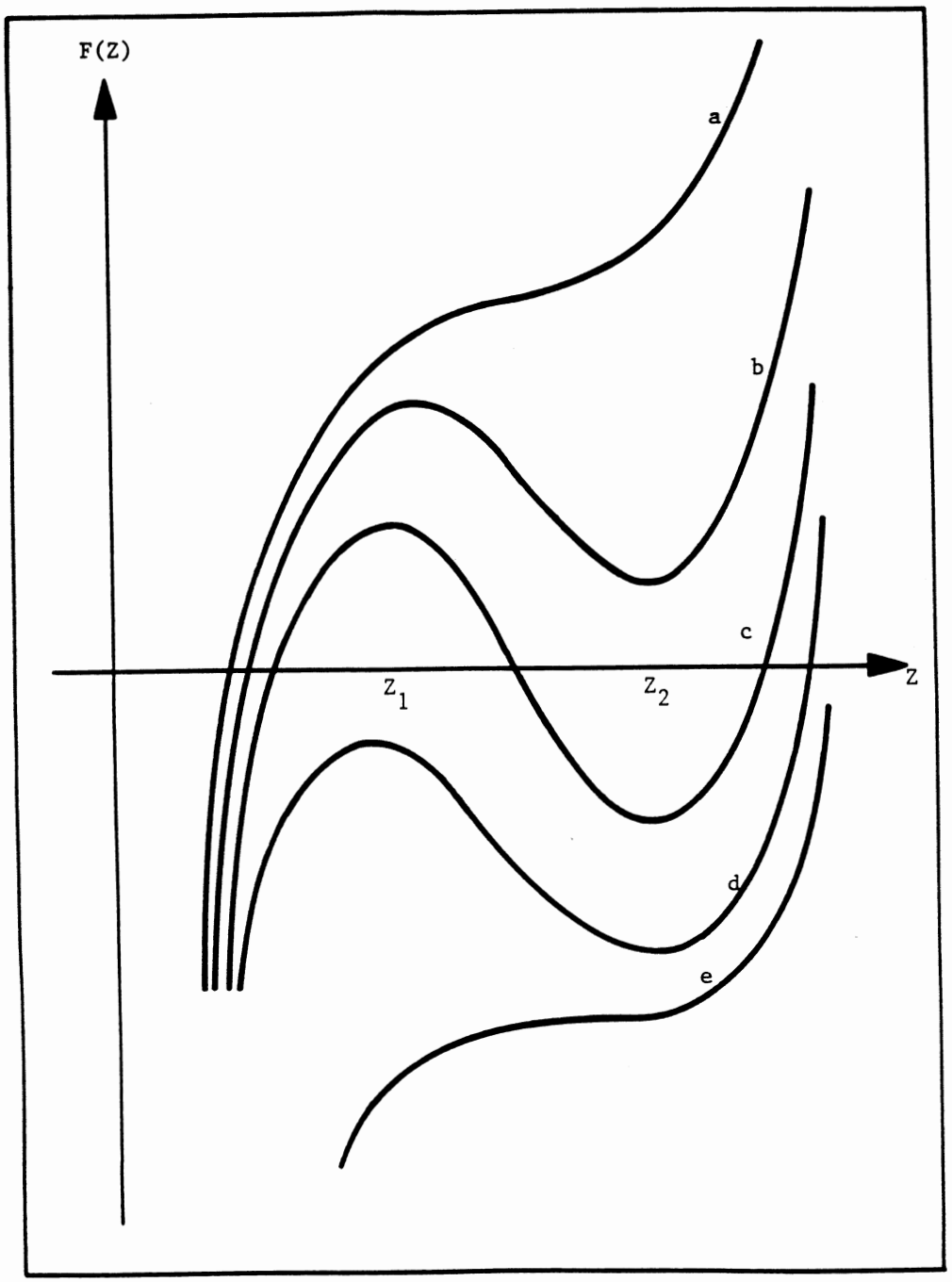

Figure 3. F(Z) Functional Behavior (Jovanovic)

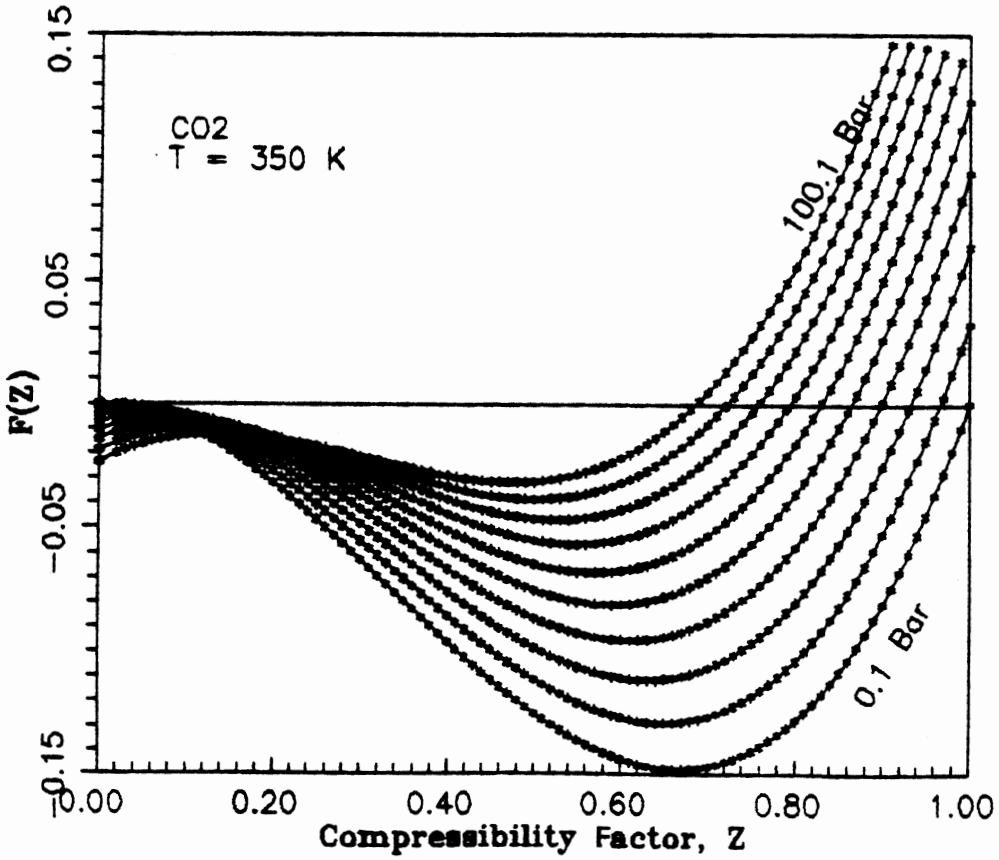

Figure 4. Compressibility Factor Mapping For PR EOS (CO_2, $T > T_c$)

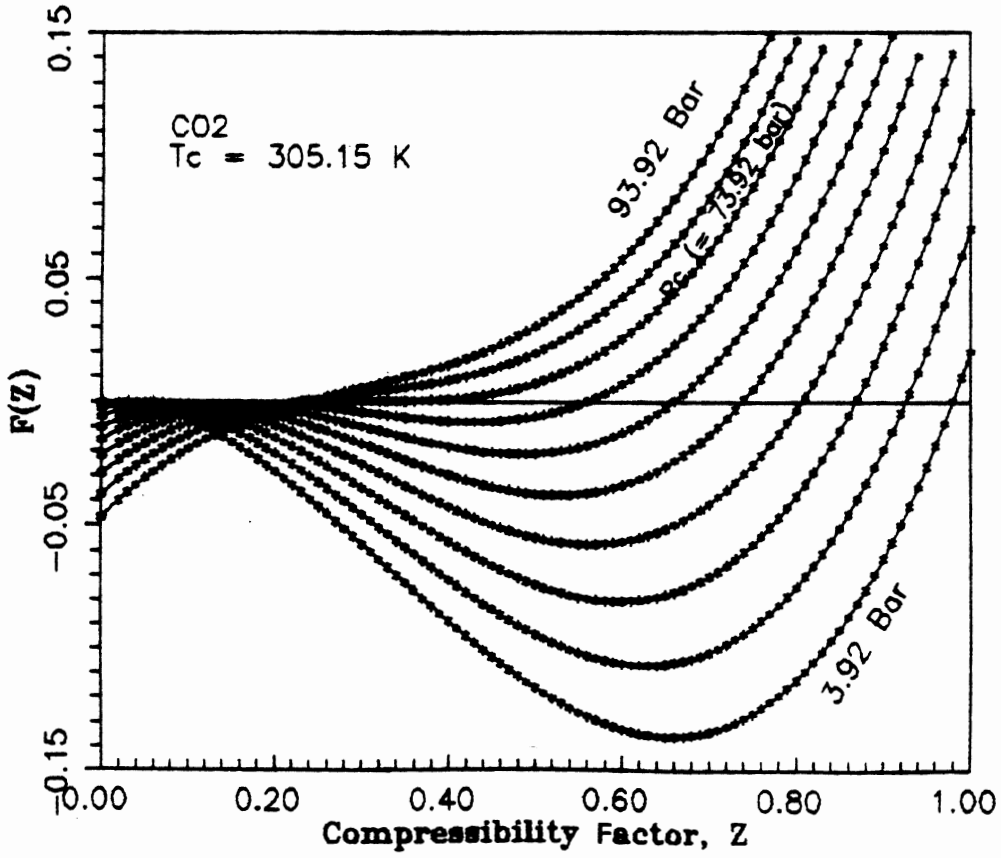

Figure 5. Compressibility Factor Mapping For PR EOS (CO_2, $T = T_c$)

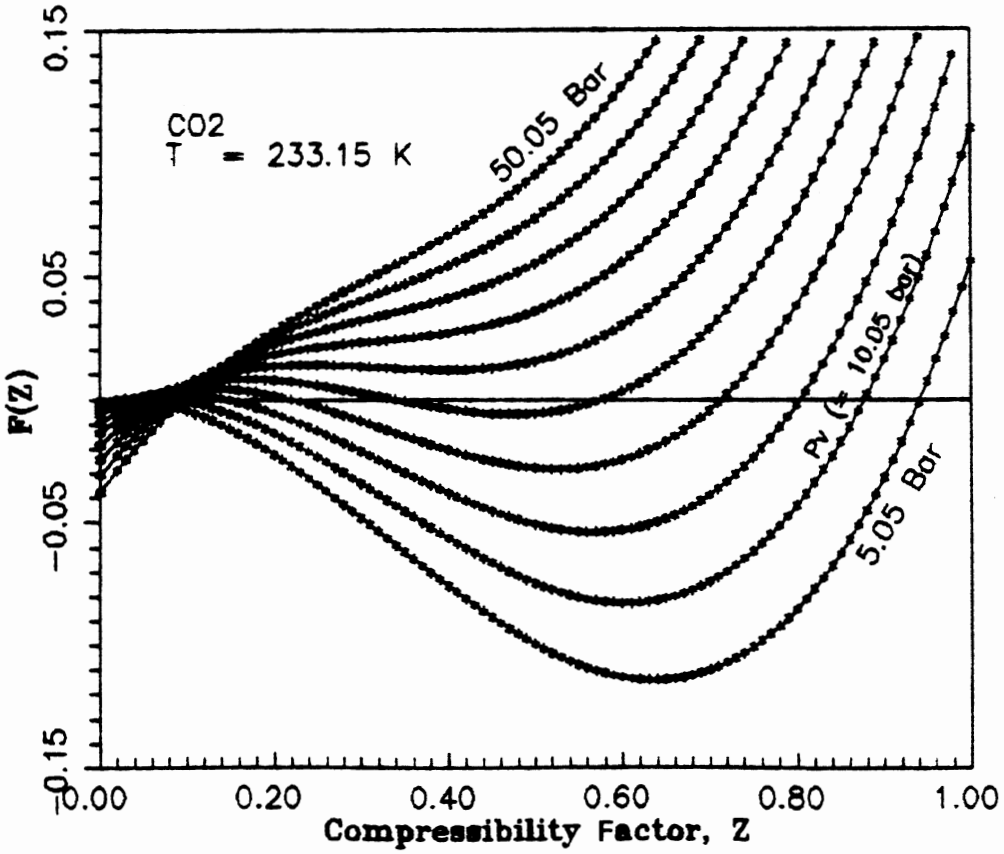

Figure 6. Compressibility Factor Mapping For PR EOS (CO_2, $T_t < T < T_c$)

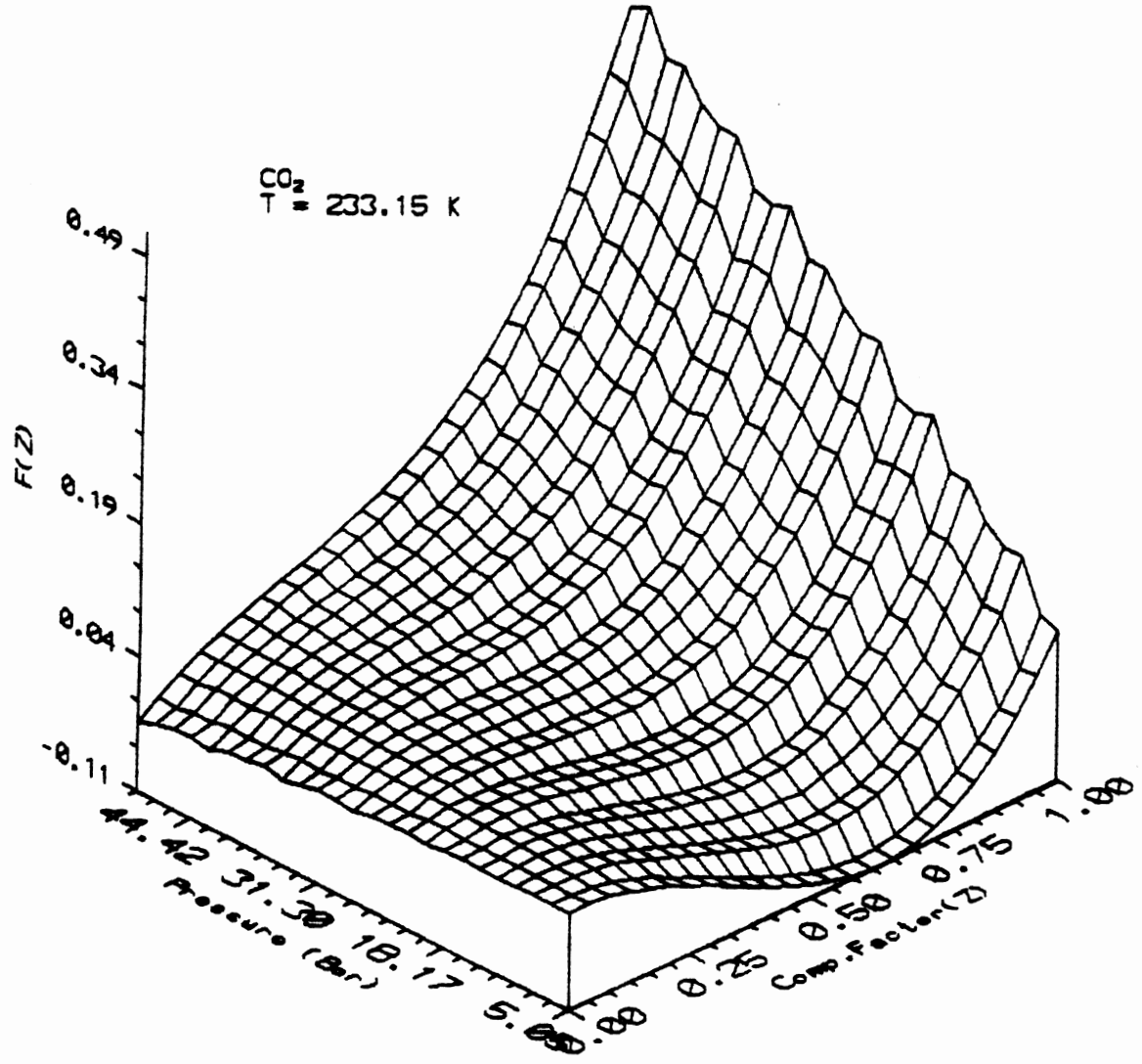

Figure 7. 3D Compressibility Factor Mapping
For PR EOS (CO_2, $T = T_c$)

The general behavior exhibited by F(Z) in Figures 4-7 will be utilized in developing an EOS solution strategy. Toward this end, the observed behavior is summarized below for the three temperature regions considered.

a. Possible F(Z) behavior for $T > T_c$

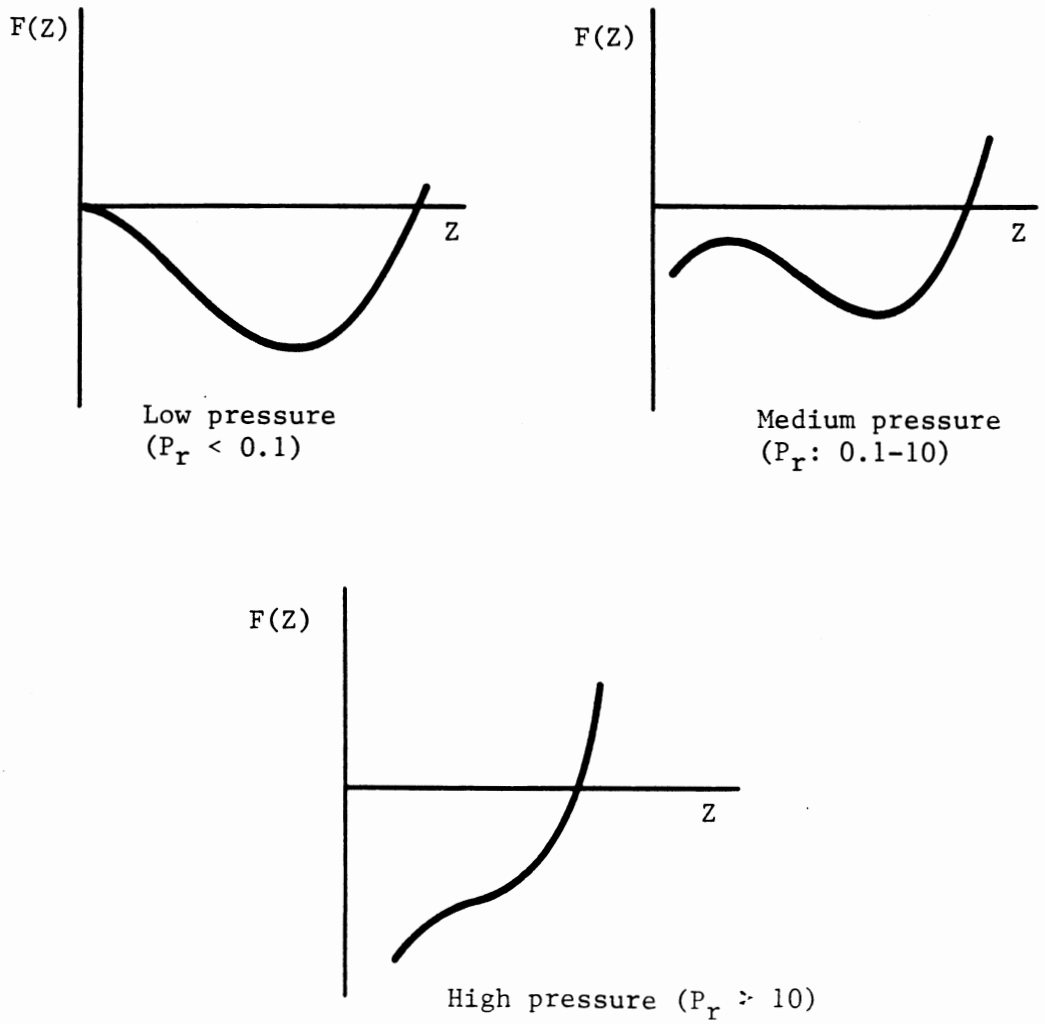

Figure 8. Possible F(Z) Forms for $T > T_c$

b. Possible F(Z) behavior for $T = T_c$

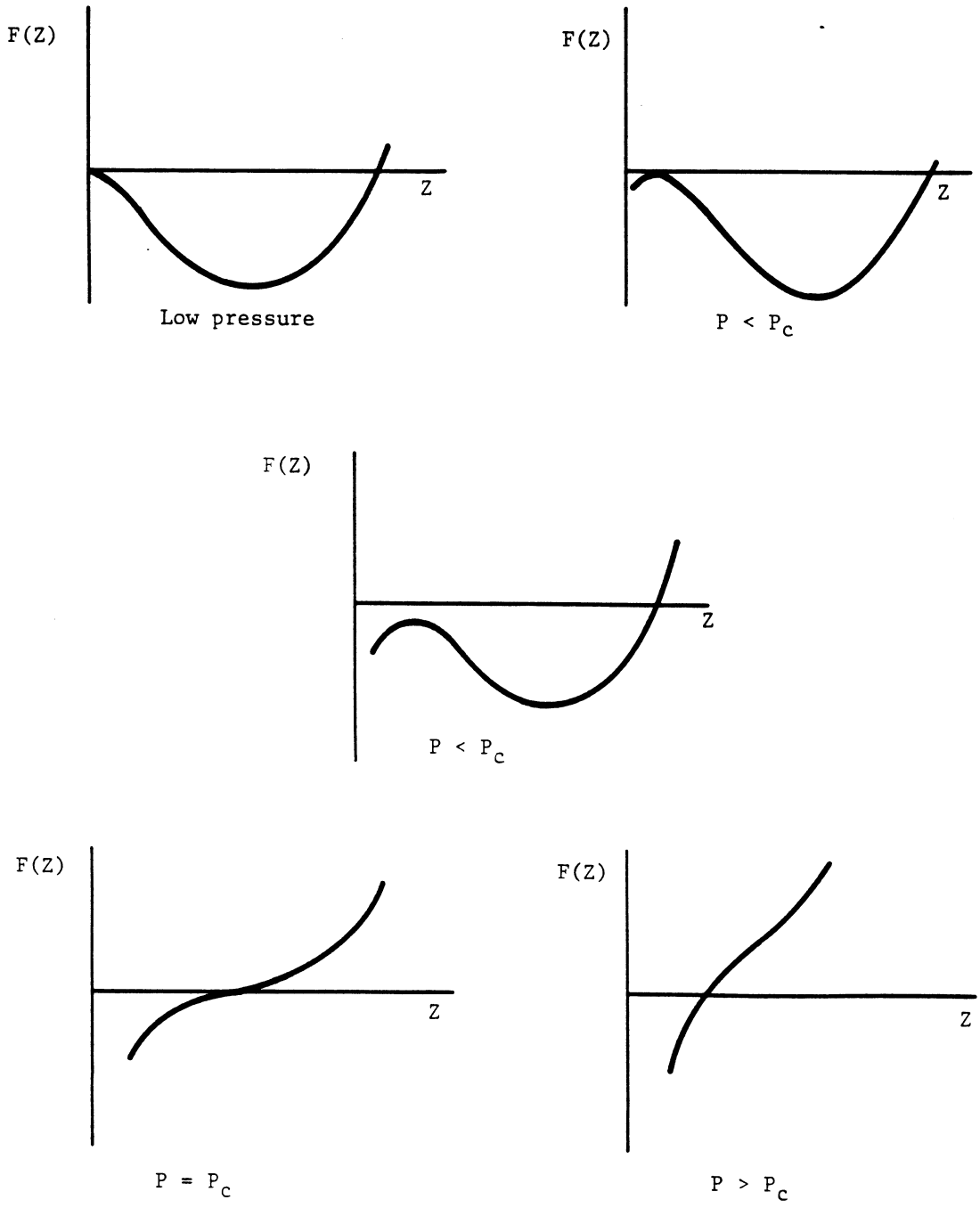

Figure 9. Possible F(Z) Forms for $T = T_c$

c. Possible F(Z) behavior for $T_c > T > T_t$

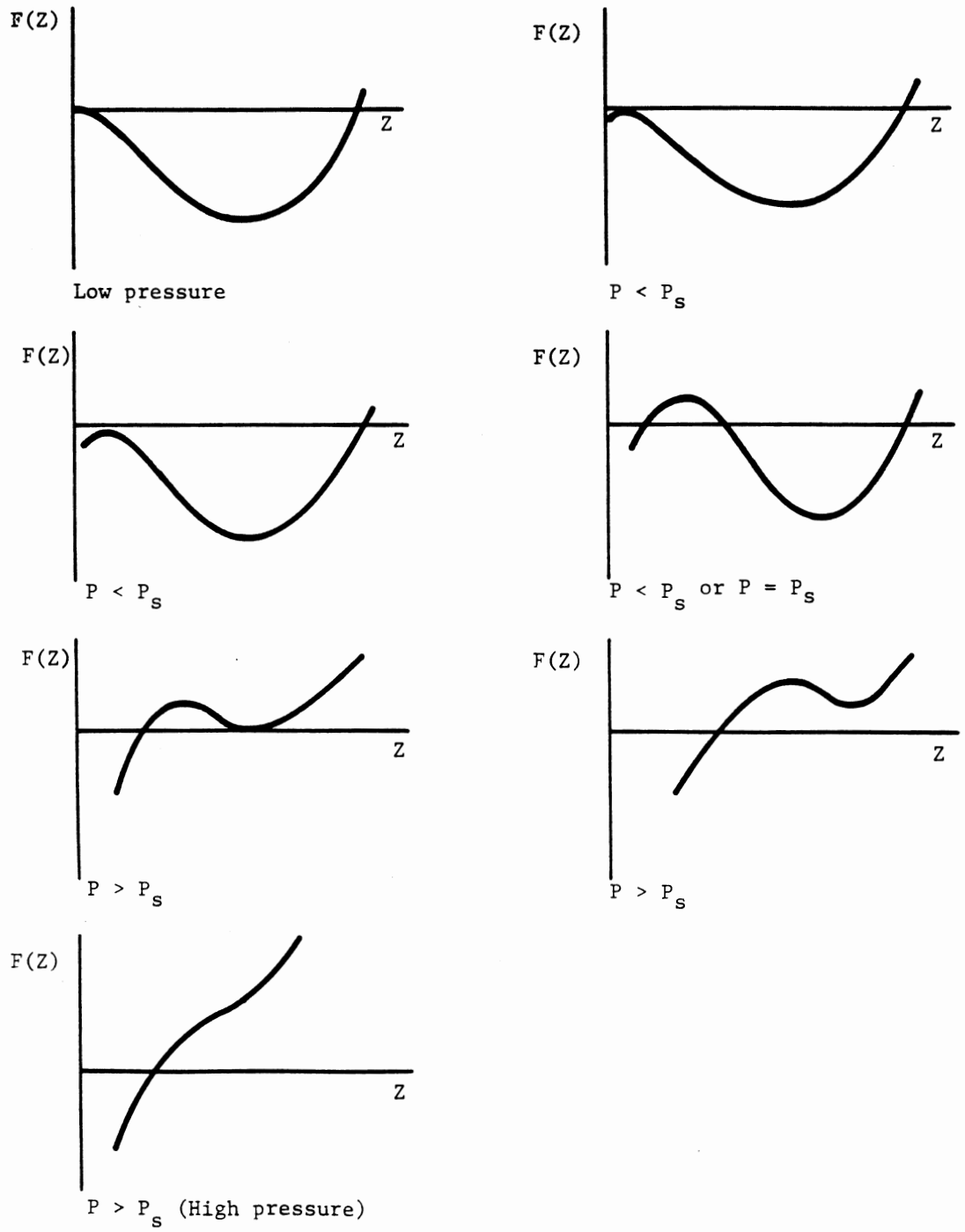

Figure 10. Possible F(Z) Forms for $T_c > T > T_t$

As indicated by Figures 8-9, while a single root will be obtained in the critical and supercritical region, at lower pressures inflection points are observed in F(Z). The functional behavior of F(Z) in the saturation region ($P = P_S$, Figure 10) is clearly distinguished by the presence of two inflection points, which result in three Z roots. Satisfying the requirement that the value of $dF/dZ > 0$ eliminates from consideration the false Z root; thus, producing two viable roots one for the liquid phase and one for the vapor phase.

From a computational point of view, the functional behavior of F(Z) can be evaluated for a set of conditions, as given by fixed values of EOS constants A and B. First, the existence of inflection points of F(Z) is evaluated. For example, when the inflection points exist at Z_1 and Z_2 of Figure 3, $F(Z_1)$ and $F(Z_2)$ are evaluated whether positive or negative. Positive $F(Z_1)$ and positive $F(Z_2)$ represent the graph shown in Figure 3b, positive $F(Z_1)$ and negative $F(Z_2)$ represent the graph shown in Figure 3c, and Figure 3a or 3e represents the case when F(Z) is free of inflection points.

Mapping F(Z) for a mixture is difficult, due to the variation in composition. However, for fixed values of the EOS constants A and B, the functional behavior of F(Z) is the same for pure fluids and mixtures. Appendix C presents a brief discussion on EOS mixing rules.

To devise a reasonable solution strategy for F(Z), the general trends observed suggest that one must (a) consider

the possible variation in the functional behavior for F(Z) as well as F'(Z), (b) provide good initial guesses, and (c) use an efficient numerical routine.

Solution Strategy

Equation (2) may be easily solved for Z by either analytical or iterative methods. Iterative methods such as the Newton-Raphson is the most commonly used in EOS applications because it is simple and converges rapidly. The formula for the Newton-Raphson method may be written as:

$$Z_{i+1} = Z_i - F(Z)/F'(Z) \qquad (8)$$

Unfortunately, Newton-Raphson is a local convergence method which will not always converge. Figure 11 illustrates such a case where this method diverges.

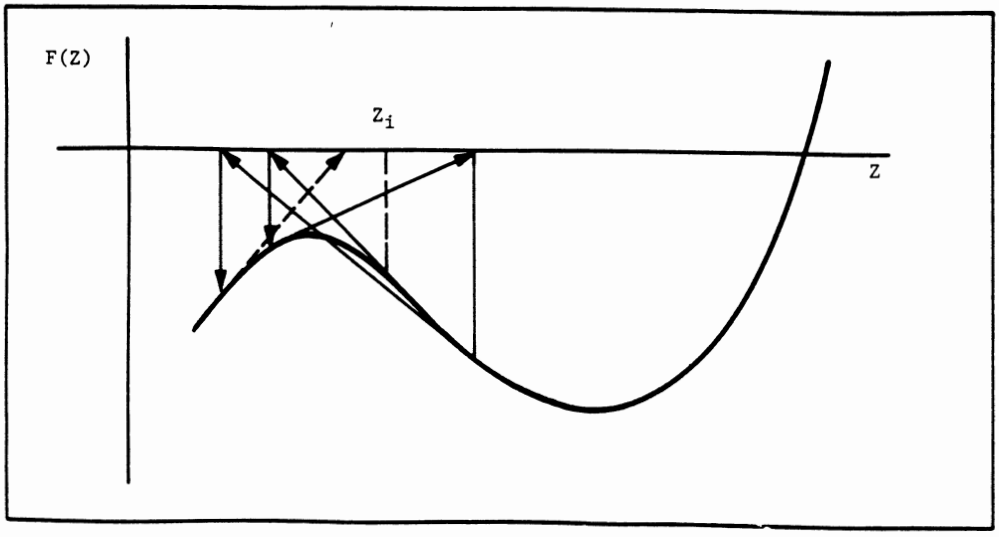

Figure 11. Newton-Raphson Method (diverging)

Other problems arise when solving the cubic EOS. For example, difficulties are encountered when the vapor compressibility factor is to be predicted from curves a or b of Figure 3. A similar situation appears for the liquid phase with Case d or e of Figure 3. If the correct root assignment cannot be achieved, equilibrium calculations can turn to the so-called "trivial solution", for which both vapor and liquid thermodynamic properties are set at the same value.

A good initial estimate for Z generally ensures convergence, minimizes the computing time, and avoids the trivial solution problem. Many strategies have been proposed to improve Z initial estimates in order to avoid these problems.

Asseleneau [3] suggested root assignment through this criteria:

For the gas phase:	Temperature must be larger than the critical temperature.
For a liquid:	Specific volume must be less than that at the critical point.

If the conditions on hand do not satisfy this criterion, a new initial estimate should be given. This scheme is not convenient and costly for repetitive computations such as those encountered in distillation.

Poling et al.[26] proposed evaluating isothermal compressibility (β) at the conditions of interest before

attempting to find the proper root for Z. An empirical criterion was proposed to assist in root assignment:

$$\text{For a liquid: } \beta < 0.005 \text{ atm}^{-1}$$

$$\text{For a vapor: } 0.9/P < \beta < 3/P$$

If this criterion is not satisfied, Poling and co-workers suggested that P, T, x, or y should be changed to generate the proper Z root, keeping the original values of P, T, x, and y for use in the phase equilibrium calculations. Specifically, they suggested to reduce pressure when vapor phase properties are desired and to increase composition of the heaviest component if liquid phase properties are desired.

A typical algorithm for flash calculations applying Poling criterion is shown in Figure 12. However, tests conducted in this study show that the upper limit for β (0.005) in the Poling criterion is not always adequate. For example, the limit of this criterion was not appropriate when applied to the CO_2 + benzene mixture. Furthermore, this criterion cannot be applied in the region near the critical point.

A method to avoid trivial solutions in bubble point pressure calculations was suggested by **Jovanovic** [17]. The method contains the following four steps:

a. Adjustment of pressure value. When close values of Z^L and Z^V (both greater then 1/3) arise, Z values should be

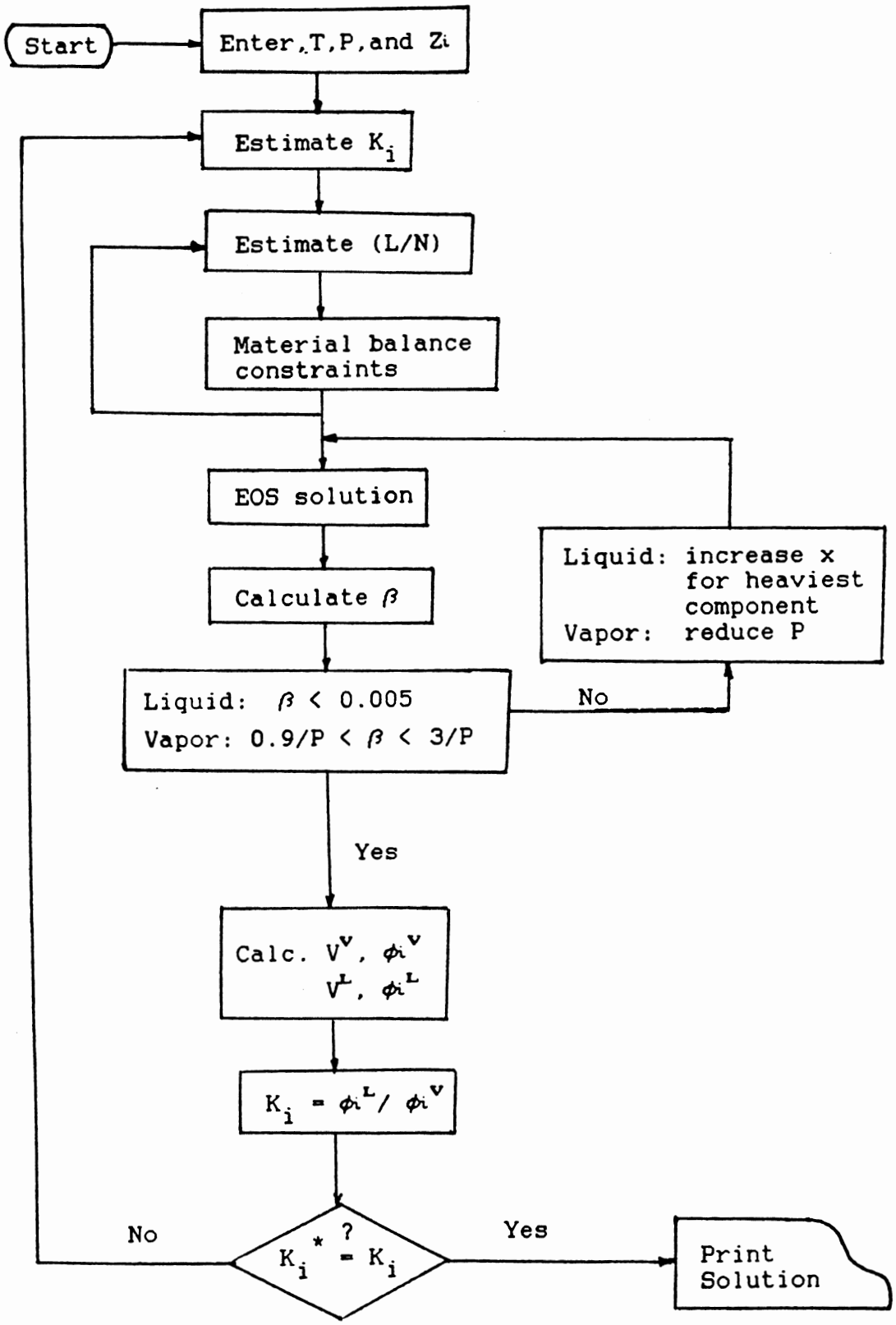

Figure 12. Flash Calculation Algorithm Using Poling Strategy

separated by gradually reducing the pressure until the condition $Z^V/Z^L > 1.2$ is met.

b. Generation of artificial density values by the local extremum Z values. The local minimum (maximum) Z value is adopted as the temporary vapor (liquid) compressibility factor. This Z value, however, should be modified slightly to prevent spurious derivative (dF/dZ) values.

c. Pressure correction to produce artificial vapor density value. The corrected pressure can be explicitly found as: $P_{cor} = RT / 3b\,(A-1)$ for SRK equation of state.

d. Temporary conservation of liquid phase density value. When Z^L leads to a "vapor like" ($Z > 1/3$) because of the pressure reduction, Z^L should be corrected: $Z^L_{new} = Z^L_{old}\, P_{cor}/P$

Edmister [10] proposed the following initial estimates:

For vapor phase: $$Z = M + \frac{F/D}{M}$$

in which $M = E/D - D$

For liquid phase: $Z = M' + B/E'M'$

in which $M' = (E'/F' + D/E')$

$E' = E/B$ and $F' = F/B^2$

These Z initial values will help in avoiding convergence problems, but do not aid in avoiding trivial solutions.

Gosset [15] proposed two approaches for root assignment. The first approach used Cardan criteria and the

second approach used criteria based on physical analogies similar to those employed by Asseleneau and Poling. In his article Gosset used the EOS constant criterion:

For vapor phase: $A/B < 5.87736$ for PR equation of state

For liquid phase: $Z < 3.9513\ B$ for PR equation of state

The algorithm proposed by Gosset involved checking for the value of F'(Z). The starting point of the iterative procedure is taken as Z = B when searching for liquid type root and Z = 1 or Z = B, whichever is least, when seeking a vapor type root (B becomes larger than one at high pressure). When the starting point is selected, a change in the sign of F'(Z) may be observed only when a single root is obtained as shown in Figure 11. When F'(Z) becomes negative the value of Z is changed so that F'(Z) is always positive; this guarantees proper solution. The Gosset algorithm can be summarized as shown in Figure 13.

Proposed Algorithm. The algorithm proposed in this study for the solution of the generalized cubic equation of state involves recognition of the F(Z) and F'(Z) forms, proper initiation and the means to avoid trivial solution. The strategy may be described as follows:

a. In case only one root exists.

If type (a) or (e) of Figure 3 is obtained, the Newton-Raphson method always converges to a single root, whatever the initial value is. If type (b) or (d) of

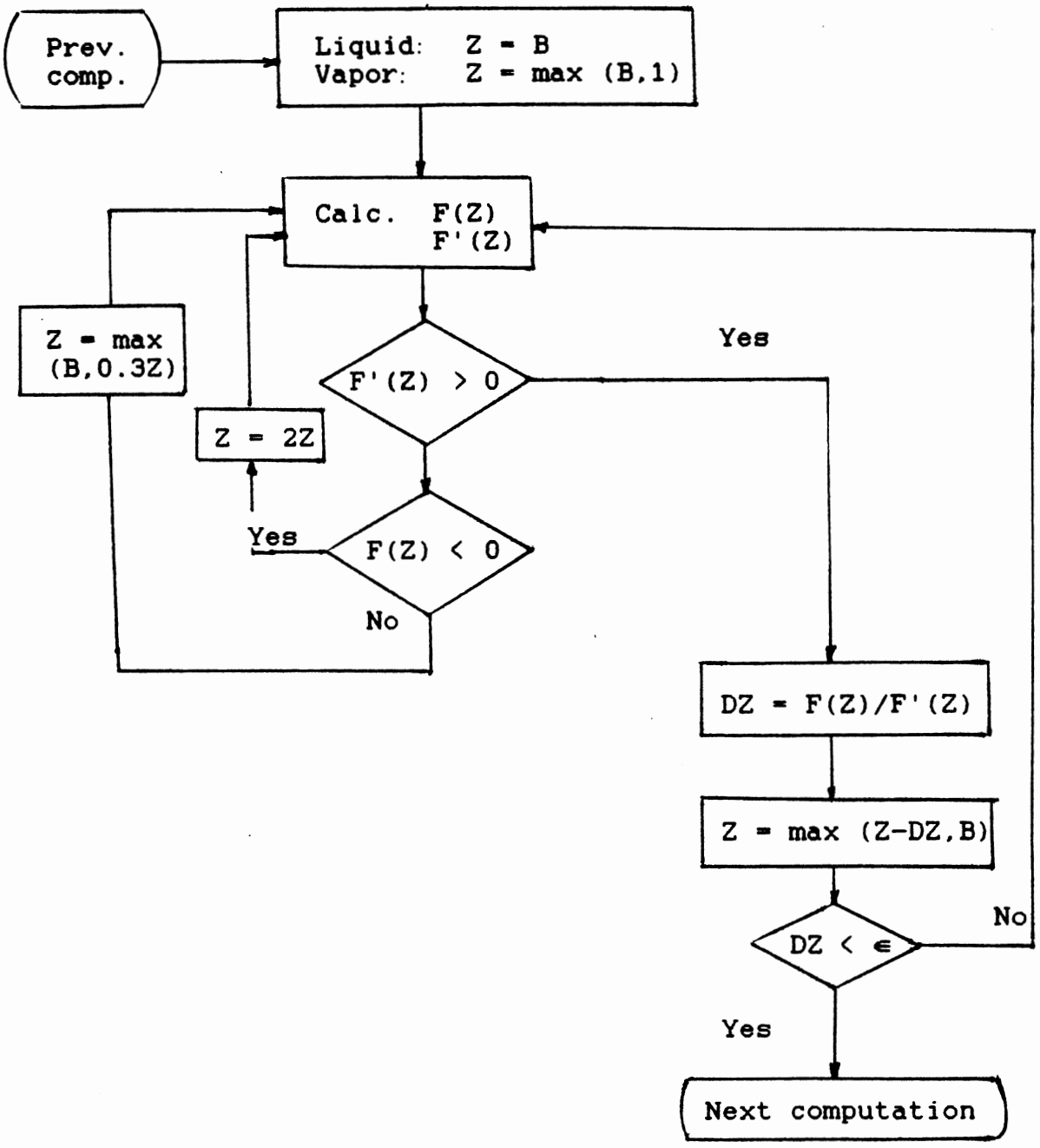

Figure 13. Gosset Algorithm for Solution of Cubic EOS

Figure 3 is obtained, initial value of Z must be chosen somewhere in between B and the inflection point Z1 (Figure 14a) for type (b) and somewhere in between one and inflection point Z2 (Figure 14b) for type a. Therefore, the inflection points should be calculated first.

The detailed algorithm for the solution of Equation (2) is as follows:

Evaluate λ: $\lambda = 4 D^2 - 12 E$

If $\lambda \leq 0$ THEN

If liquid root is evaluated: Zi = 1.01 B

If vapor root is evaluated: Zi = 1.0

Else, evaluate Z1, Z2, FZ1 and FZ2:

$Z1 = (-2 D - \lambda^{0.5})/6$

$Z2 = (-2 D + \lambda^{0.5})/6$

$FZ1 = Z1^3 + D Z1^2 + E Z1 - F$

$FZ2 = Z2^3 + D Z2^2 + E Z2 - F$

If liquid root is evaluated and FZ1 >0: Zi = (Z1+B)/2.0

If liquid root is evaluated and FZ1 <0: Zi = (Z2+1.0)/2.0

If vapor root is evaluated and FZ2 <0: Zi = (Z1+1.0)/2.0

If vapor root is evaluated and FZ2 >0: Zi = (Z2+B)/2.0

An alternative method for obtaining the desired roots (which was not implemented in this study) is to take the optimum values of Z obtained from the derivative of F(Z) as a temporary compressibility factor. Accordingly, Z2 can be used as a temporary vapor compressibility factor and Z1 can be used as a temporary liquid compressibility factor when

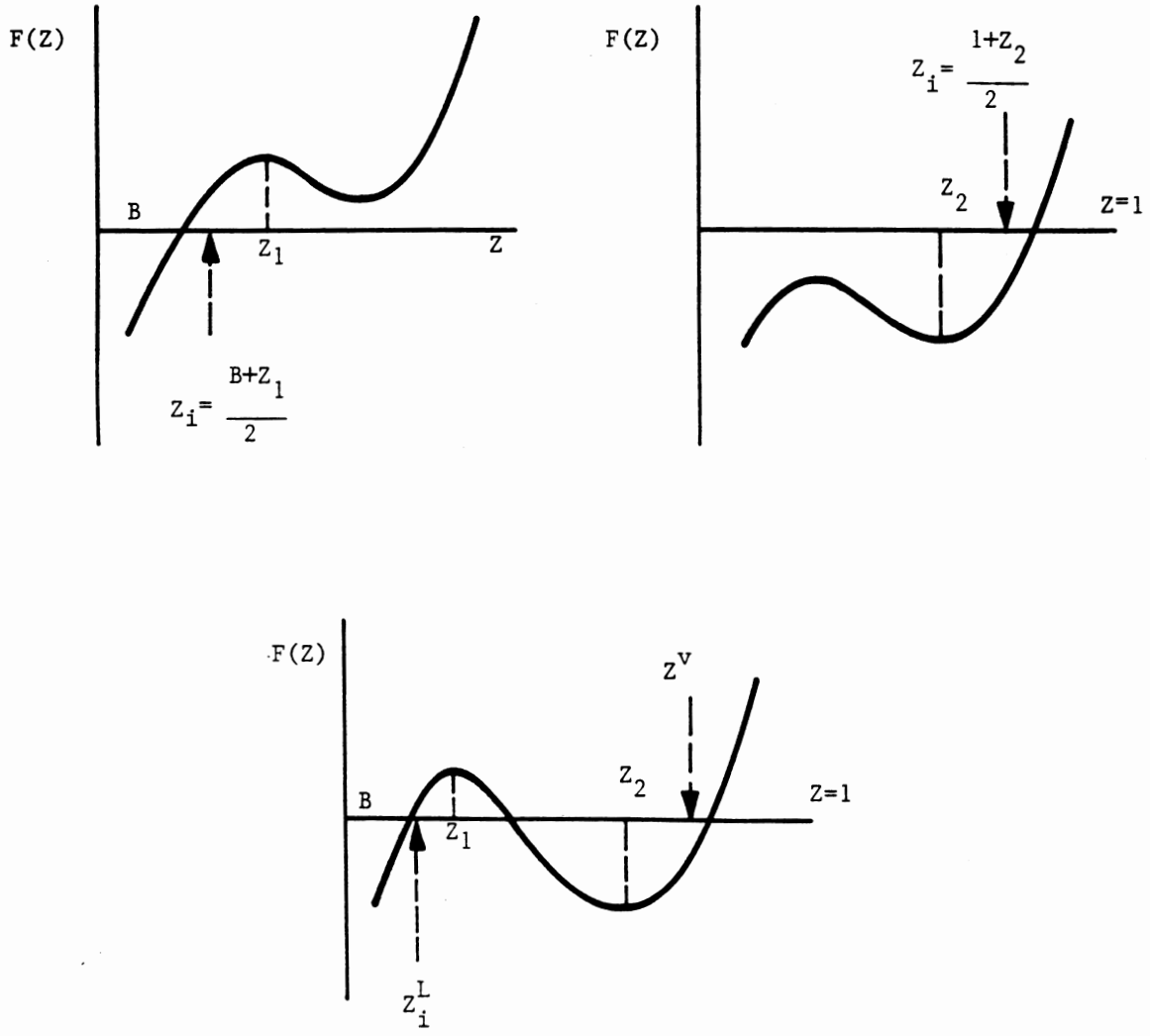

Figure 14. Initial Estimates for Z

the real values cannot be achieved. In this case, the procedure becomes:

If $\lambda \leq 0$ then

For liquid phase: If $F(Z1) \geq 0$: $Z_i = (Z1 + B)/2$

If $F(Z1) < 0$: $Z_{calc} = Z1$

For vapor phase: If $F(Z2) > 0$: $Z_{calc} = Z2$

If $F(Z2) \leq 0$: $Z_i = (1 + Z2)/2$

b. In case three roots exist

When type (c) of Figure 3 is obtained, the initial estimate described above is still valid (Figure 14c) but at high pressure, this strategy may result in a root that is less than B [33]. Therefore, the initial estimate must be increased until positive value of F'(Z) is obtained.

c. Avoiding trivial roots

Poling strategy can be applied to avoid trivial solutions but care must be taken concerning the limits of the β criterion. Tests conducted on the CO_2 + benzene mixture show that a better β criterion for the liquid phase is $\beta < 0.03$ instead of $\beta < 0.005$. Furthermore, this criterion, as expected, is not suitable in the region near the critical point. In this case, a *stair-casing* procedure should be used.

To facilitate application of Poling's procedure with various cubic equations of state, an expression for $\beta(Z)$ for the generalized cubic EOS was derived:

$$\beta = -\left(\partial V/\partial P\right)_T / V \qquad (9)$$

$$= -\frac{1}{P}\left[1 + \frac{\{(uB-B)Z^2 + (2wB^2-2uB^2-uB+A)\,Z - (3wB^3+2wB^2+2AB)\}}{\{\,Z\,(3Z^2+2(uB-B-1)\,Z + (wB^2-uB^2-uB+A)\,\}}\right]$$

The proposed algorithm for the solution of the generalized equation of state (GEOS) is presented in Figure 15 (Poling procedure is not included). Several systems have been used to test the validity of this solution strategy. In addition, this algorithm has been successfully used in all our evaluation of EOS density predictions presented next.

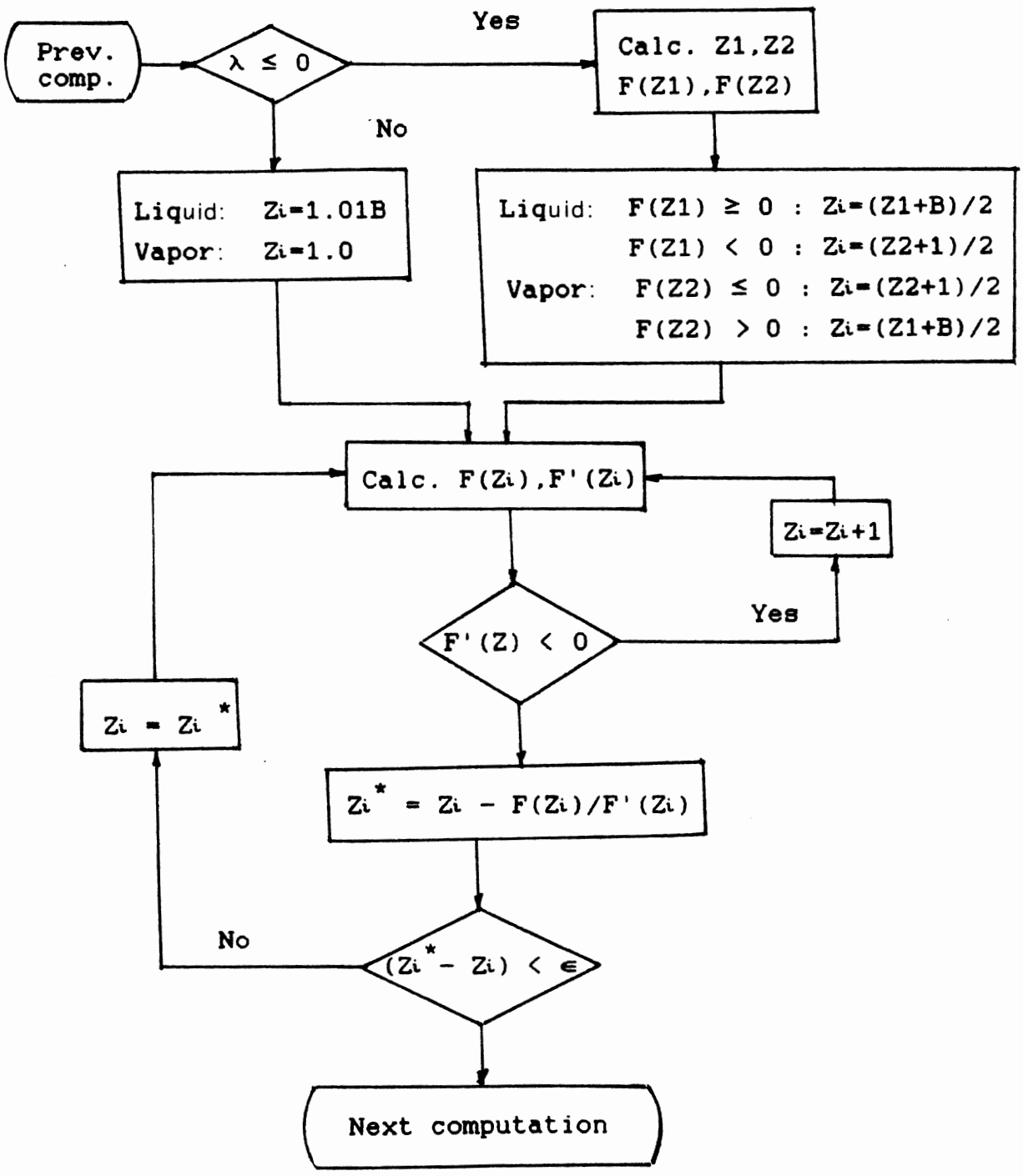

Figure 15. The Algorithm for GEOS Solution

CHAPTER III

QUALITY OF EOS VOLUMETRIC PREDICTIONS FOR CO_2 + HYDROCARBON SYSTEMS

Original SRK and PR Equations of State

Mixture density predictions have been performed using the strategy discussed in the previous chapter. To assess the quality of the EOS predictions, experimental phase density measurements acquired at the OSU [see, e.g., 13] for CO_2 + hydrocarbon binaries were employed in our evaluation. The hydrocarbons include n-butane, n-decane, n-tetradecane, cyclohexane, trans-decalin and benzene. The predictions cover the reduced pressure range from approximately 0.6 to near the critical.

To calculate the phase densities of mixtures, the equation of state constants a and b are calculated using the following mixing rules [14]:

$$a = \sum_i \sum_j z_i z_j \, (a_{ii} a_{jj})^{1/2} \, (1 - C_{ij}) \qquad (10)$$

and

$$b = \sum_i \sum_j z_i z_j \left(\frac{b_{ii} + b_{jj}}{2}\right)(1 + D_{ij}) \qquad (11)$$

where z is mole fraction; a_{ii}, a_{jj}, b_{ii} and b_{jj} are pure component parameters; and C_{ij} and D_{ij} are binary interaction

parameters; $C_{ii} = C_{jj} = 0$ and $D_{ii} = D_{jj} = 0$. See Appendix C for more details.

Several cases were employed to evaluate the density predictions using the EOS approach, as described in Table II. The results given in Table III for Case 1 indicate that while the original PR EOS gives better liquid density predictions in comparison to the SRK and RK EOS (6.4 % AAD), the SRK EOS gives better vapor density predictions (10.7 % AAD). As expected, Figure 16 shows that for most hydrocarbons the cubic EOS density predictions tend to be worse as the pressure moves towards the critical point.

Significant improvement has been realized when the binary interaction parameters are fitted with the experimental data. Table IV presents the results for Case 2, where the binary interaction parameters C_{ij} is fitted and D_{ij} is set to zero (3.4 and 3.2 % AAD for the liquid and the vapor densities using PR EOS). Table V shows the results when both the binary interaction parameters are fitted (Case 3). Predictions within 1.4 and 2.2 % AAD are obtained from the PR EOS for the liquid and vapor densities, respectively. In general, the RK EOS and the SRK EOS give less accurate predictions than those of the PR EOS in both Cases 2 and 3. Optimum interaction parameters for the systems considered are given in Table B.1 (Appendix B).

Translated-Volume Predictions

When applied to both vapor and liquid phases, equations

TABLE II

DESCRIPTION OF CASES USED TO EVALUATE THE CUBIC EOS METHOD

Case	Description
	---------- EOS Without Volume translation ----------
1	RK, SRK and PR EOS $C_{ij} = D_{ij} = 0$
2	RK, SRK and PR EOS C_{ij} regressed , $D_{ij} = 0$
3	RK, SRK and PR EOS C_{ij} and D_{ij} are regressed.
	---------- EOS With Volume translation ----------
4	Original Peneloux (Equations 15 & 16) a) RK & SRK EOS: $a_1 = 0.44943$ $a_2 = 0.29441$ PR EOS: $a_1 = 0.30483$ $a_2 = 0.29441$ b) PR EOS: $a_1 = 0.30483$ $a_2 = 0.24240$
5	Peneloux (Equations 15 & 16) a) PR EOS: a_1 and a_2 regressed simultaneously for liquid and vapor density. b) PR EOS: a_1 and a_2 regressed separately for liquid and vapor density.

TABLE II (Continued)

Case	Description
6	Peneloux (Equations 15 & 16) PR EOS: a_1 and a_2 are generalized.
7	Proposed model (Equation 36) a) PR EOS: A_1 and A_2 are regressed simultaneously for liquid and vapor density. b) PR EOS: A_1 and A_2 are regressed separately for liquid and vapor density.
8	Proposed model (Equation 36) a) PR EOS: A_1 is regressed simultaneously for liquid and vapor density, A_2 is set constant. b) PR EOS: A_1 is regressed separately for liquid and vapor density, A_2 is set constant.
9	Proposed model (Equation 36) PR EOS, A_1 and A_2 are generalized.

TABLE III

SATURATED DENSITY PREDICTION USING CUBIC EOS
WITHOUT VOLUME TRANSLATION
Case 1: Cij & Dij = 0

Mixture CO_2 +	No Pts	EOS	% AAD	
			Liquid	Vapor
n-Butane	42	RK	6.62	21.05
		SRK	5.23	17.21
		PR	8.27	22.03
n-Decane	40	RK	17.66	3.52
		SRK	12.46	2.56
		PR	3.00	3.03
n-Tetra-decane	17	RK	24.57	10.43
		SRK	17.97	8.14
		PR	8.80	4.45
Benzene	16	RK	5.16	25.81
		SRK	3.90	16.26
		PR	10.20	24.00
c-Hexane	14	RK	4.01	25.19
		SRK	2.87	16.84
		PR	10.30	24.26
t-Decalin	20	RK	12.47	9.83
		SRK	10.09	6.82
		PR	1.08	8.44
Overall Statistics:		RK	12.01	14.52
		SRK	8.91	10.71
		PR	6.35	13.52

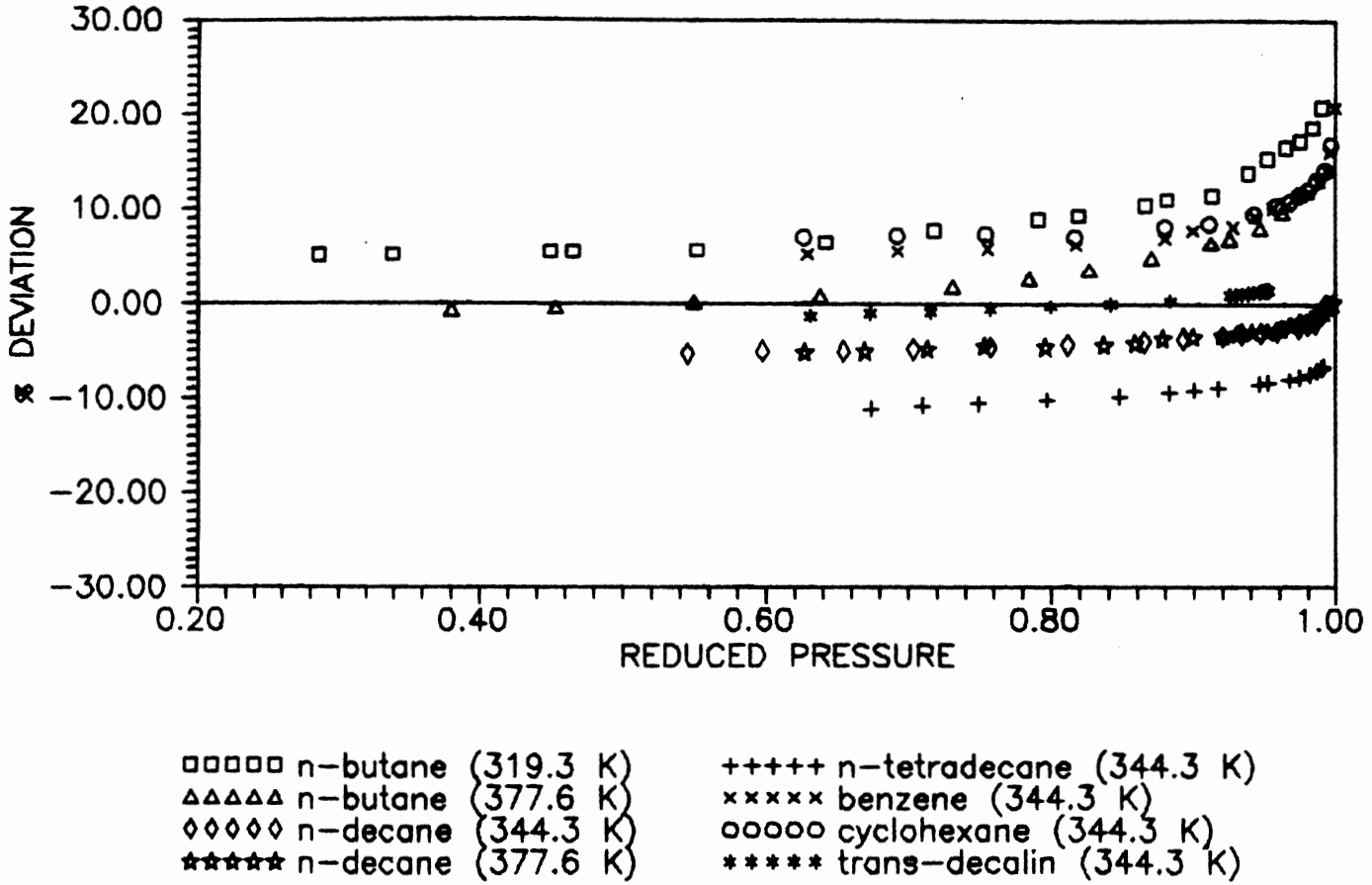

Figure 16a. Saturated Liquid Density Predictions Using Original PR EOS Without Interaction Parameters

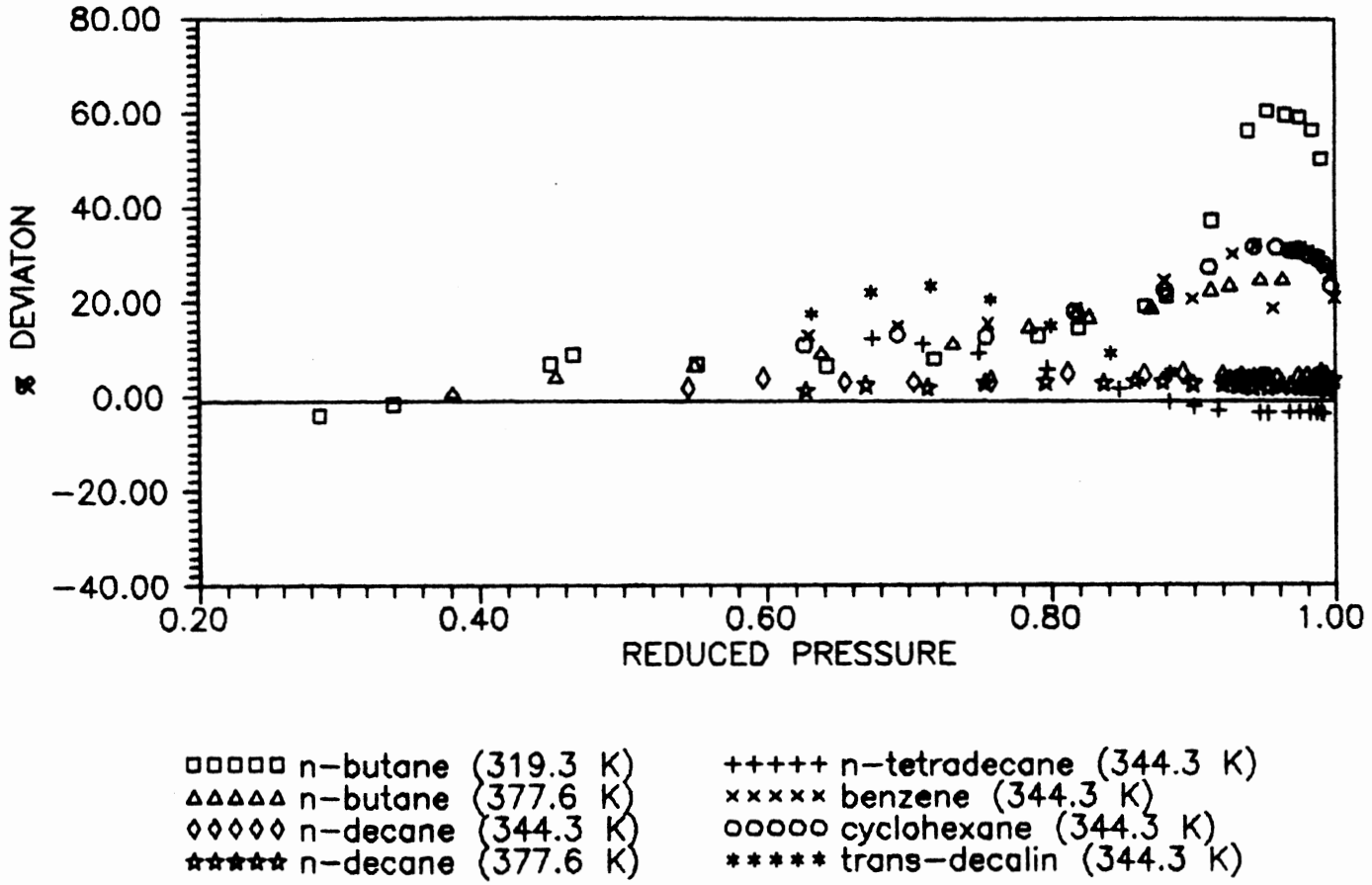

Figure 16b. Saturated Vapor Density Predictions Using Original PR EOS Without Interaction Parameters

TABLE IV

SATURATED DENSITY PREDICTION USING CUBIC EOS WITHOUT VOLUME TRANSLATION
Case 2: Cij REGRESSED, Dij = 0

Mixture CO_2 +	No Pts	EOS	% AAD	
			Liquid	Vapor
n-Butane	42	RK	11.50	3.96
		SRK	8.62	2.66
		PR	2.63	2.38
n-Decane	40	RK	13.66	7.57
		SRK	8.65	3.49
		PR	3.44	2.46
n-Tetra-decane	17	RK	17.76	8.51
		SRK	13.13	4.79
		PR	7.13	3.71
Benzene	16	RK	11.49	7.05
		SRK	7.56	4.40
		PR	2.75	3.90
c-Hexane	14	RK	11.29	6.67
		SRK	7.37	4.09
		PR	3.05	3.63
t-Decalin	20	RK	12.46	9.44
		SRK	9.24	6.30
		PR	2.49	4.79
Overall Statistics:		RK	12.90	6.77
		SRK	8.99	3.94
		PR	3.39	3.16

TABLE V

SATURATED DENSITY PREDICTION USING CUBIC EOS WITHOUT VOLUME TRANSLATION
Case 3: Cij & Dij REGRESSED

Mixture CO_2 +	No Pts	EOS	% AAD	
			Liquid	Vapor
n-Butane	42	RK	3.13	3.10
		SRK	2.33	2.43
		PR	1.86	1.31
n-Decane	40	RK	1.47	1.76
		SRK	1.39	1.40
		PR	0.38	1.02
n-Tetra-decane	17	RK	0.72	5.36
		SRK	1.18	2.98
		PR	0.59	3.40
Benzene	16	RK	2.23	2.19
		SRK	0.93	1.60
		PR	2.38	3.04
c-Hexane	14	RK	2.51	2.03
		SRK	1.26	1.00
		PR	2.97	2.95
t-Decalin	20	RK	1.50	6.19
		SRK	1.16	3.95
		PR	1.07	4.50
Overall Statistics:		RK	2.04	3.21
		SRK	1.54	2.20
		PR	1.37	2.24

of state can be used to calculate all the equilibrium thermodynamic properties of pure fluids and mixtures. However, as illustrated by the results above, cubic equations of state show moderate success in calculating phase densities, especially without EOS tuning. Modifications involving the translation concept have been proposed to improve EOS density prediction [7,20,25]. The proposed models lead to corrections in the predicted densities without affecting the equilibrium property prediction (fugacity).

Translation along the volume axis

Translation along the volume axis was first introduced by Martin [20] who proposed the following general cubic equation of state:

$$P = \frac{RT}{V} - \frac{\alpha(T)}{(V+\beta)(V+\gamma)} + \frac{\delta(T)}{V(V+\beta)(V+\gamma)} \qquad (12)$$

Other equations of state might be related to this equation. For example, Redlich-Kwong equation of state

$$P = \frac{RT}{V-b} - \frac{a}{V(V+b)} \qquad (13)$$

can be obtained by translating the volume in Equation (12) by t, and then letting $t = \beta = b$, $\gamma = 2t = 2\beta$, $\alpha = a$, and $\delta = 0$. One can also set $\delta = 0$, translate by $\beta+t$ in volume, and let $\beta = b$, $\gamma = \beta$, and $\alpha = a$ to get:

$$P = \frac{RT}{(V-tb)} - \frac{a}{(V-t)^2} \qquad (14)$$

which is the equation recommended by Martin.

The EOS constants, α , β, and γ can be evaluated by the classical method of van der Waals, where the first two pressure-volume derivatives vanish at the critical point.

Following the work of Martin, simple volume translation has been implemented by Peneloux [25], where

$$V = V^{model} - \Sigma\, c_i\, x_i \qquad (15)$$

$$c_i = a_1 \left(\frac{RTc_i}{Pc_i} \right) \left(a_2 - ZRA_i \right) \qquad (16)$$

$$b = b^{model} - \Sigma\, c_i\, x_i \qquad (17)$$

a_1 and a_2 are regressed model parameter, and b is the cubic equation of state constant. Matching experimental saturated liquid densities at $T_r = 0.7$ for n-alkanes up to n-decane, Peneloux determined the values of a_1 and a_2 for SRK equation of state as 0.40768 and 0.29441, respectively. Refitting a_1 and a_2 specifically for CO2 + n-paraffin liquid densities, Gasem [12] obtained $a_1 = 0.44943$ for the SRK and $a_1 = 0.30483$ for the PR equation of state.

Rackett compressibility factor, ZRA, from Spencer and Danner [31] is used in Equation (16). However values of ZRA from other sources such as Hankinson and Thomson [16] can also be used.

Even though the volume translation models suggested above clearly produces improved density predictions, these models cannot remove the large discrepancy between measured and calculated saturated liquid densities near the critical point.

In 1988 Chou and Prausnitz corrected this deficiency. A "distance" variable was introduced in the volume translation in order to locate the correct critical point. Once volume translation locates the true critical point, a "nonclassical" contribution is added to the residual Helmholtz energy to account for density fluctuations near the critical point.

Volume translation introduced by Prausnitz is expressed as:

$$V = V^{model} - c - \delta_c \left[\frac{\eta}{\eta + d} \right] \tag{18}$$

where c is the constant of translation used by Peneloux and η is a universal constant that has a value of 0.35. Volume shift at the critical temperature, δ_c, is given by:

$$\delta_c = \frac{RT_c}{P_c} \left(Z_c^{SRK} - Z_c \right) \tag{19}$$

The true residual Helmholtz energy was assumed equal to the sum of a classical contribution and a nonclassical contribution:

$$a^r = a^C + a^{NC} \tag{20}$$

where a^C was obtained by integrating the volume-translated SRK equation. a^{NC} was evaluated using the following expression:

$$\frac{a^{NC}}{RT_c} = a_m^{NC} \exp(-wD^2) \tag{21}$$

where a_m^{NC} is a constant representing the maximum nonclassical contribution at the true critical point and w is a constant reflecting how fast the function decays as a system moves away from the true critical point. These values are 7×10^{-4} and 90, respectively. D is a dimensionless distance variable defined as:

$$D = \frac{1}{\rho} \left(\frac{\partial P^{SRK-VT}}{\partial \rho} \right)_T \left(\frac{\rho_c}{RT_c} \right) \tag{22}$$

Equation (18) might be extended to mixtures as:

$$V = V^{model} - \sum x_i c_i - \delta_{cm} \left(\frac{\eta}{\eta + d_m} \right) \tag{23}$$

where d_m is defined:

$$d_m = \frac{1}{RT_{cm}} \left(\frac{\partial P^{SRK}}{\partial \rho} \right)_T - \left(\frac{1}{RT_{cm} \rho^2} \right) \frac{a_{\nu 1}^2}{a_{11}} \tag{24}$$

and

$$\delta_{cm} = V_{cm}^{model} - V_{cm} - \sum x_i c_i \tag{25}$$

V_{cm}^{model} is the mixture critical volume predicted from SRK equation and V_{cm} is the true critical volume evaluated using a correlation proposed by Chueh and Prausnitz in 1967 [10]:

$$V_{cm} = \Sigma\, \theta_i V_{ci} + \Sigma\Sigma\, \theta_i \theta_j \nu_{ij} \tag{26}$$

where ν_{ij} is a binary parameter characteristic of the i-j interaction, and θ_i is the surface fraction of i defined by:

$$\theta_i = \frac{x_i V_{ci}^{2/3}}{\Sigma\, x_i V_{ci}^{2/3}} \tag{27}$$

To account for density fluctuations near the critical point, the same nonclassical Helmholtz energy as that for pure fluids was proposed by Chou et al. [7]. In this case, however, T_c is replaced by mixture critical temperature T_{cm} and D is replaced by D_m defined by:

$$D_m = \frac{\rho_{cm}}{RT_{cm}\rho}\left[\left(\frac{\partial P^{SRK-VT}}{\partial \rho}\right)_T - \frac{1}{\rho^2}\frac{a_{\nu 1}^2}{a_{11}}\right] \tag{28}$$

The results reported on a number of pure liquids and mixtures, using the corrected SRK equation indicate that for pure liquids volume translation not only locates the correct critical point, but also significantly improves liquid density predictions over a wide temperature range [7]. Volume translation has a much smaller effect on vapor density. On the mixture density predictions, the nonclassical correction does not have an appreciable effect,

since the binary parameters C_{ij} and D_{ij} have more profound influence.

Peneloux's volume translation strategy has been evaluated in this study. In doing so, the interaction parameters C_{ij} and D_{ij} are set to zero, a_1 = 0.44943 and a_2 = 0.29441 for the RK and the SRK EOS and a_1 = 0.30483 and a_2 = 0.29441 for PR EOS.

When the original Peneloux's parameters are used (Case 4), the SRK EOS gave about 4.7 % AAD for liquid predictions and 11.5 % AAD for vapor density predictions. The PR EOS gave about 12 % AAD for liquid density predictions and 16 % AAD for the vapor predictions. These PR EOS predictions are worse than those of the original PR EOS without interaction parameters, implying that the parameters a_1 or a_2 are not optimum. Several evaluations have been conducted showing that refitting a_1 does not improve the predictions. However, refitting a_2 for PR EOS gave better results (5 % AAD for liquid predictions and 11 % AAD for vapor predictions).

The results are improved when parameters a_1 and a_2 are fitted (Case 5), as shown in Table VII for the PR EOS predictions. In Case 5a, where a_1 and a_2 are regressed simultaneously for liquid and vapor, the results did not show significant improvement compared to Case 4. However when liquid and vapor density predictions are optimized separately, measurable improvements have been achieved. In this case (Case 5b), the liquid predictions gave

TABLE VI

SATURATED DENSITY PREDICTIONS USING CUBIC EOS
WITH PENELOUX'S VOLUME TRANSLATION
(Case 4)

Mixture CO_2 +	No Pts	EOS	Case A* % AAD		Case B** % AAD	
			Liquid	Vapor	Liquid	Vapor
n-Butane	42	RK	4.98	23.82	-	-
		SRK	4.38	19.58	-	-
		PR	12.76	23.82	4.57	19.06
n-Decane	40	RK	7.16	5.70	-	-
		SRK	0.93	1.19	-	-
		PR	6.71	5.74	6.33	0.92
n-Tetra-decane	17	RK	8.81	7.34	-	-
		SRK	1.49	4.05	-	-
		PR	6.27	4.83	8.61	5.90
Benzene	16	RK	4.73	29.97	-	-
		SRK	5.12	19.82	-	-
		PR	15.62	26.75	4.24	19.75
c-Hexane	14	RK	3.87	29.23	-	-
		SRK	5.36	20.34	-	-
		PR	15.85	26.95	3.38	20.03
t-Decalin	20	RK	11.09	11.45	-	-
		SRK	14.97	8.67	-	-
		PR	20.63	15.59	2.99	5.59
Overall Statistics:		RK	6.69	16.58	-	-
		SRK	4.72	11.50	-	-
		PR	12.05	16.30	5.14	11.05

* For RK/SRK: $a_1 = 0.44943$ $a_2 = 0.29441$
PR: $a_1 = 0.30483$ $a_2 = 0.29441$

** PR: $a_1 = 0.30483$ $a_2 = 0.24240$

TABLE VII

SATURATED DENSITY PREDICTIONS USING PR EOS
WITH PENELOUX'S VOLUME TRANSLATION
(Case 5)

Mixture CO_2 +	No Pts	Case A* % AAD		Case B** % AAD	
		Liquid	Vapor	Liquid	Vapor
n-Butane	42	10.33	13.49	4.29	3.35
n-Decane	40	1.10	0.77	0.45	0.48
n-Tetra-Decane	17	0.80	3.82	0.19	3.38
Benzene	16	6.37	5.41	1.87	3.75
c-Hexane	14	6.44	4.75	1.13	2.67
t-Decalin	20	1.51	5.40	0.05	3.21
Overall Statistics:		4.79	6.20	1.67	2.54

* a_1 & a_2 regressed simultaneously for liquid and vapor

** a_1 & a_2 regressed separately for liquid and vapor

approximately 1.7 % AAD and the vapor predictions gave 2.5 % AAD.

Inspection of the optimum values of a_1 and a_2 obtained reveals wide variation among the different solvents, which indicates a possible difficulty in parameter generalization. This assessment is validated by the results of the simple parameter generalizations undertaken. Table VIII summarizes the results for Case 6, where common values of a_1 and a_2 are used for all the systems considered, as suggested by Peneloux. The quality of the generalized predictions (4.6 and 7.6 % AAD for the liquid and vapor densities, respectively) signify the need for a better procedure for parameter generalization.

Figure 17 depicts the relative deviations obtained for the PR EOS with and without volume translation. While volume translation affects improvements in the density prediction, similar patterns are observed for the relative deviations.

Scaled-volume translation

Another model that has proven capable of predicting a full saturation density range using volume translation is one developed utilizing the scaling-law behavior [14]. This model introduced a density correction factor by employing the following deviation function:

$$\theta = \frac{PV}{(PV)^{model}} \qquad (29)$$

TABLE VIII

SATURATED DENSITY PREDICTION USING PR EOS
WITH PENELOUX'S VOLUME TRANSLATION
Case 6: a_1 & a_2 GENERALIZED

Mixture CO_2 +	No Pts	% AAD	
		Liquid	Vapor
n-Butane	42	4.58	6.85
n-Decane	40	3.41	10.11
n-Tetra-decane	17	6.14	11.43
Benzene	16	4.33	4.31
c-Hexane	14	3.51	3.72
t-Decalin	20	6.47	6.49
Overall Statistics:		4.57	7.63

* a_1 = 0.38103 & a_2 = 0.25006 for liquid
a_1 = 3.25654 & a_2 = 0.25659 for vapor

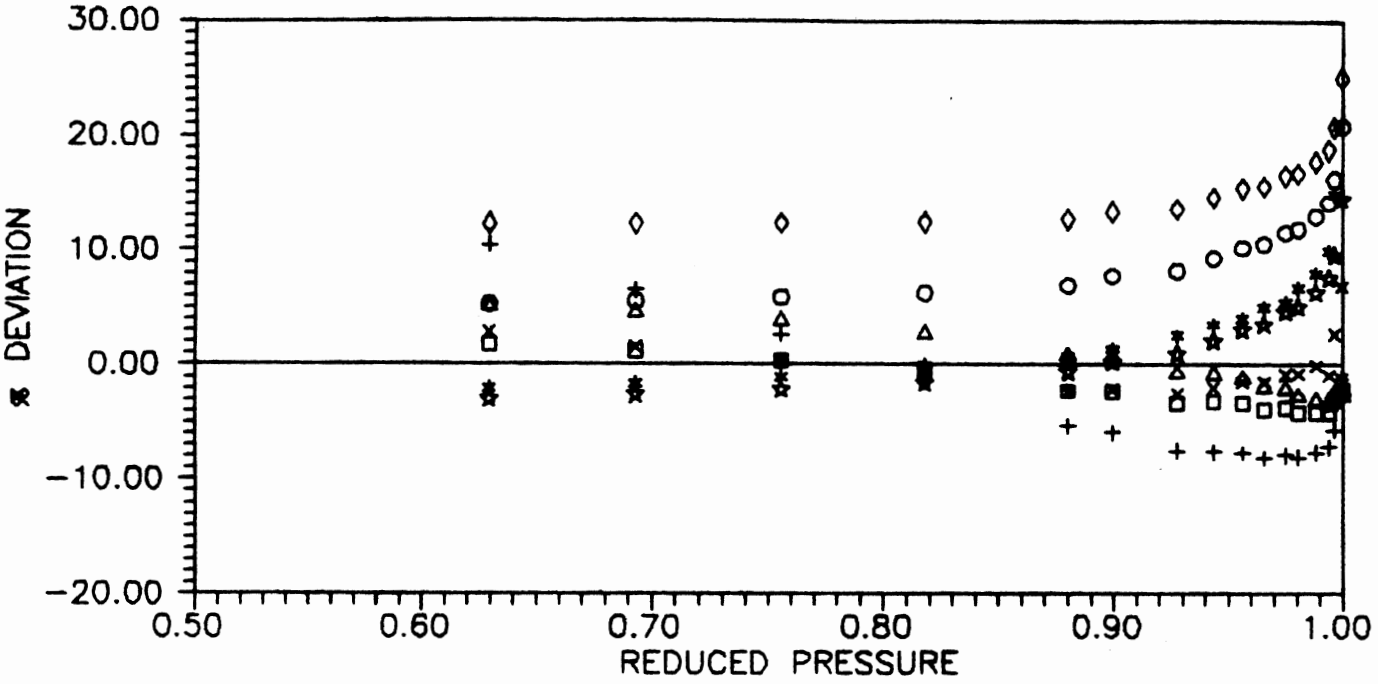

Figure 17a. Saturated Liquid Density Predictions for CO_2 + Benzene at 344.3 K Using PR EOS

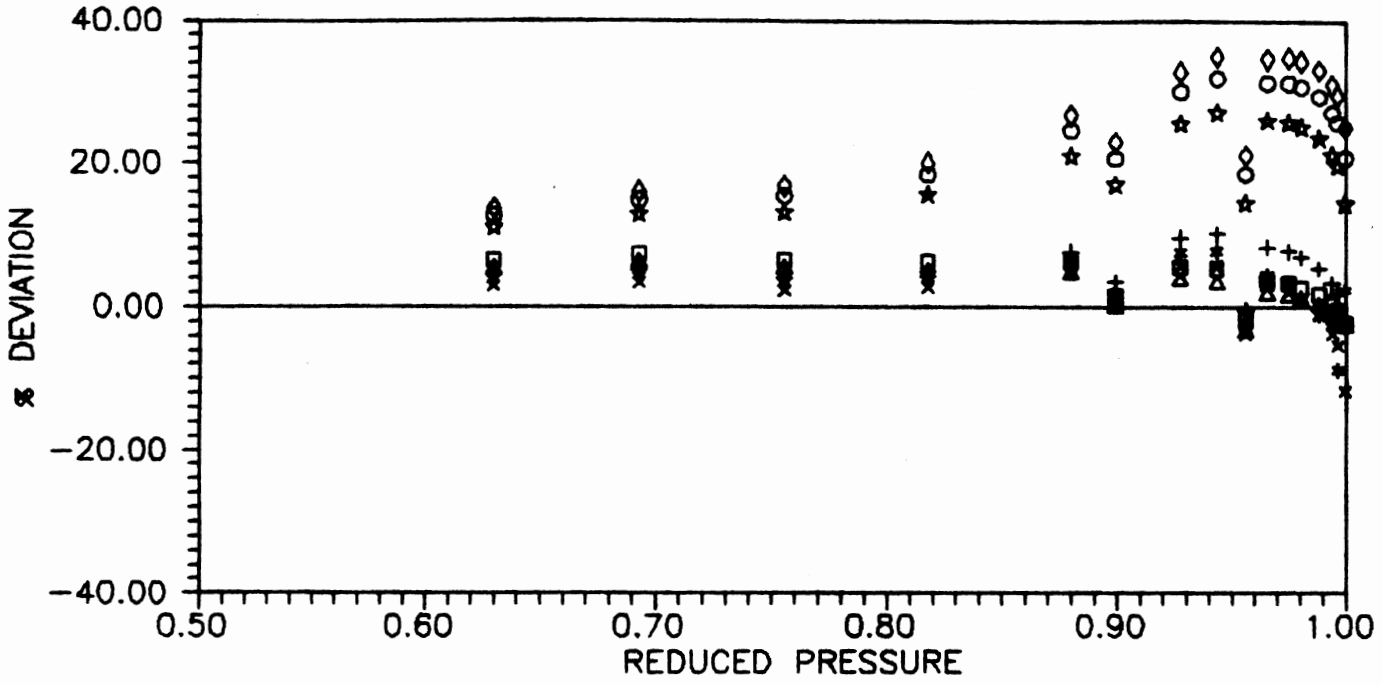

Figure 17b. Saturated Vapor Density Predictions for CO_2 + Benzene at 344.3 K Using PR EOS

Applied specifically to the EOS model, the correction factor is:

$$\theta_{EOS} = \frac{PV}{(PV)_{EOS}} \tag{30}$$

or $$\theta = \rho_{EOS} / \rho \tag{31}$$

for a constant pressure volume translation.

A simple definition of θ which will provide for reasonable approximation of the scaling-law behavior may be inferred from the following arguments.

The phase densities of a given mixture may be represented by the following extended scaling-law expression:

$$\phi_{\pm} = \phi_c + A_o \varepsilon^{1-\alpha} + \sum_{j=1}^{M} A_j (\varepsilon)^j \pm 1/2 \sum_{i=0}^{N} B_i (\varepsilon)^{\beta+i\Delta} \tag{32}$$

where ϕ is saturation property α, β and Δ are universal constants which have the value 1/8, 1/3, and 1/2, respectively [6]. The liquid and vapor phases are represented by + and - sign, respectively. A_j and B_i are parameters dependent on the system. In general, one may extend the series as needed to fit the experimental data. Charoensombut-Amon used M = 3 and N = 6, Dulcamara [9] used M = 6 and N = 6, and Gasem [13] pointed that it is sufficient to truncate the series at M = 3 and N = 5 for liquid density predictions.

Application of Equation (32) to phase density

prediction leads to the following limiting expression:

$$(\rho/\rho_c)_{exp} = 1 \pm A\,\varepsilon^{\beta} + \ldots\ldots \text{ as } \varepsilon \text{ ----> } 0 \qquad (33)$$

for the experimental data. For a cubic EOS, equivalent representation is given by:

$$(\rho/\rho_c)_{EOS} = 1 \pm A\,\varepsilon^{\Delta} + \ldots\ldots \text{ as } \varepsilon \text{ ---> } 0 \qquad (34)$$

where β is approximately 1/3 and Δ is 0.5.

Utilizing Equation (33) in deriving an expression for θ is inconvenient, since it contains too many parameters. Accordingly, a correlation function offered by the Scaled-Variable-Reduced-Coordinate (SVRC) approach is used for this purpose. The SVRC approach [30] which will be discussed further in the next chapter suggests the following simple relation for θ

$$\theta \;\alpha\; A^{\varepsilon^{\beta}} \qquad (35)$$

Comparison between Equation (31), (33), (34) and (35) suggests the following translation strategy:

$$(\rho/\rho_c)_{exp} = (\rho/\rho_c)_{EOS}\;\; A^{\varepsilon^{\beta-\Delta}}$$

or $$\rho = \rho_{EOS}\left(\frac{\rho_{c\_exp}}{\rho_{c\ EOS}}\right)\;\; A^{\varepsilon^{\beta-\Delta}}$$

or $$\rho = \rho_{EOS}\;\; A_1\, A_2^{\varepsilon^{\beta-\Delta}} \qquad (36)$$

A_1 and A_2 can be evaluated by matching experimental saturated phase densities and ε is defined as:

$$\varepsilon = \frac{P_c - P}{P_c - P_t} \qquad (37)$$

in which P_t is the lowest pressure of the experimental data.

Application of this model to the CO_2 + hydrocarbon systems under study gave minor improvement when A_1 and A_2 are regressed simultaneously for liquid and vapor densities, as given by Case 7 of Table IX. However, excellent results are achieved when A_1 and A_2 for liquid and vapor density predictions are regressed separately. As shown in Table IX, for the PR EOS liquid density predictions result in about 0.7 % AAD and the vapor predictions give about 2.7 % AAD.

The optimum parameters A_1 and A_2 for Cases 7-8 (given in Tables B.4 and B.5) are of similar value for the systems considered. This promises to provide for simple generalizations; a fact disputed by the results presented in Tables X and XI for the generalized-parameter predictions.

Sensitivity of the translation model to the values of A_1 and A_2 combined with the simple generalization strategy used result in marked loss of accuracy (6.2 and 10.2 % AAD for liquid and vapor, respectively) for Case 9 in comparison to Cases 7 and 8.

Figures 18a and 18b show the relative error distributions for liquid and vapor predictions using the scaled-volume translation. In general, these figures

TABLE IX

SATURATED DENSITY PREDICTIONS USING PR EOS
WITH SCALED-VOLUME TRANSLATION
(Case 7)

Mixture CO_2 +	No Pts	T, K	Case A* % AAD		Case B** % AAD	
			Liquid	Vapor	Liquid	Vapor
n-Butane	18	319.26	7.15	7.26	0.44	5.88
	12	344.26	5.62	4.83	0.16	2.12
	12	377.59	5.36	4.95	0.16	1.72
n-Decane	17	344.26	3.43	3.70	0.52	0.16
	23	377.59	2.68	2.52	1.02	0.48
n-Tetra-decane	17	344.26	5.20	4.39	2.00	3.84
Benzene	16	344.26	6.39	6.19	0.88	4.23
c-Hexane	14	344.26	6.39	6.31	0.19	4.23
t-Decalin	20	344.26	3.89	3.57	0.17	2.33
Overall Statistics:			4.96	4.71	0.66	2.71

* A_1 & A_2 regressed simultaneously for liquid and vapor

** A_1 & A_2 regressed separately for liquid and vapor

TABLE X

SATURATED DENSITY PREDICTIONS USING PR EOS
WITH SCALED-VOLUME TRANSLATION
(Case 8)

Mixture CO_2 +	No Pts	T, K	Case A* % AAD		Case B** % AAD	
			Liquid	Vapor	Liquid	Vapor
n-Butane	18	319.26	8.86	16.76	3.87	17.15
	12	344.26	6.28	9.94	3.37	9.06
	12	377.59	5.71	7.38	2.89	6.10
n-Decane	17	344.26	3.42	3.70	0.50	1.22
	23	377.59	2.70	2.51	1.41	0.48
n-Tetra-decane	17	344.26	5.21	4.40	1.77	4.95
Benzene	16	344.26	6.74	6.38	3.05	4.08
c-Hexane	14	344.26	6.49	7.44	2.11	5.15
t-Decalin	20	344.26	4.04	4.09	0.82	5.36
Overall Statistics:			5.31	6.66	2.08	5.71

* A_1 regressed simultaneously for liquid and vapor
$A_2 = 1.0$

** A_1 regressed separately for liquid and vapor
$A_2 = 1.0$

TABLE XI

SATURATED DENSITY PREDICTION USING PR EOS
WITH SCALED-VOLUME TRANSLATION
Case 9: A_1 & A_2 GENERALIZED

Mixture CO_2 +	No Pts	T, K	% AAD	
			Liquid	Vapor
n-Butane	18	319.26	7.88	16.66
	12	344.26	5.51	9.16
	12	377.59	2.01	5.42
n-Decane	17	344.26	6.19	9.40
	23	377.59	5.67	10.65
n-Tetra-decane	17	344.26	11.83	12.62
Benzene	16	344.26	6.72	8.12
c-Hexane	14	344.26	6.84	8.66
t-Decalin	20	344.26	2.91	8.65
Overall Statistics:			6.24	10.19

* A_1 = 1.00588 & A_2 = 0.980197 for liquid
  A_1 = 0.904191 & A_2 = 0.980341 for vapor

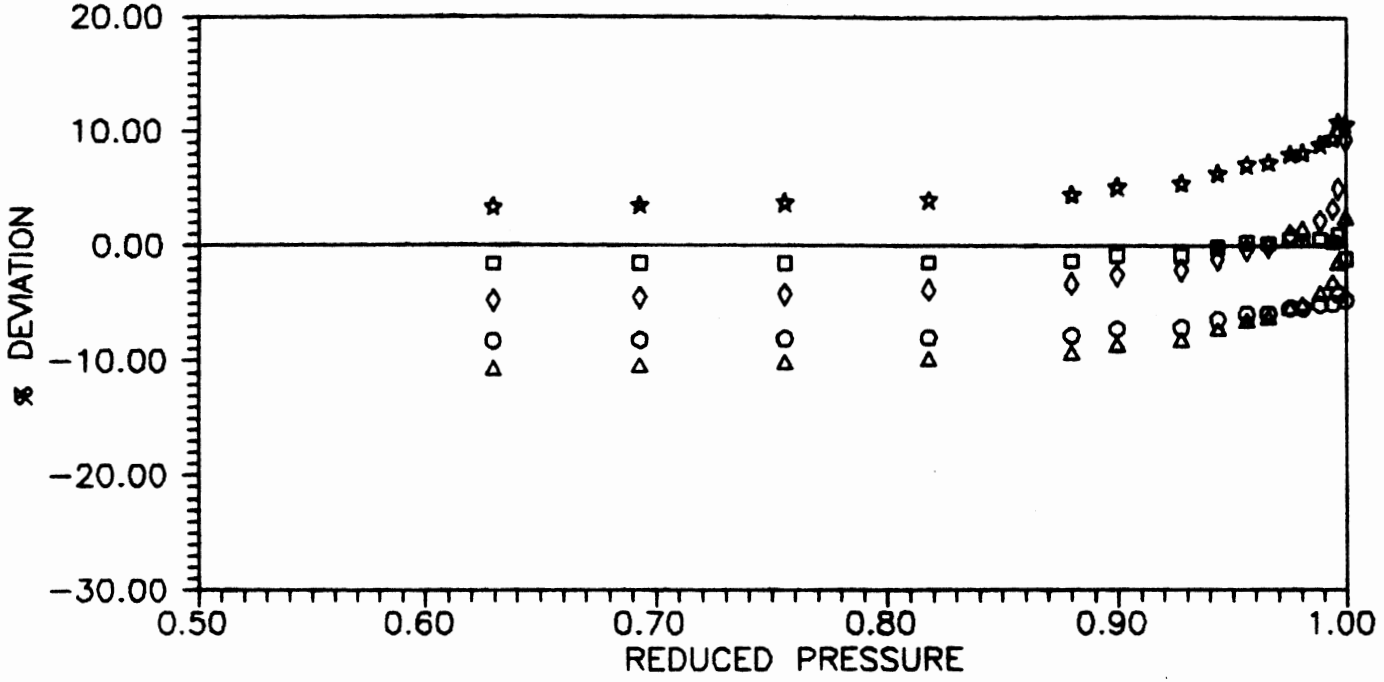

Figure 18a. Saturated Liquid Density Predictions for CO_2 + Benzene at 344.3 K Using PR EOS with Scaled-Volume Translation

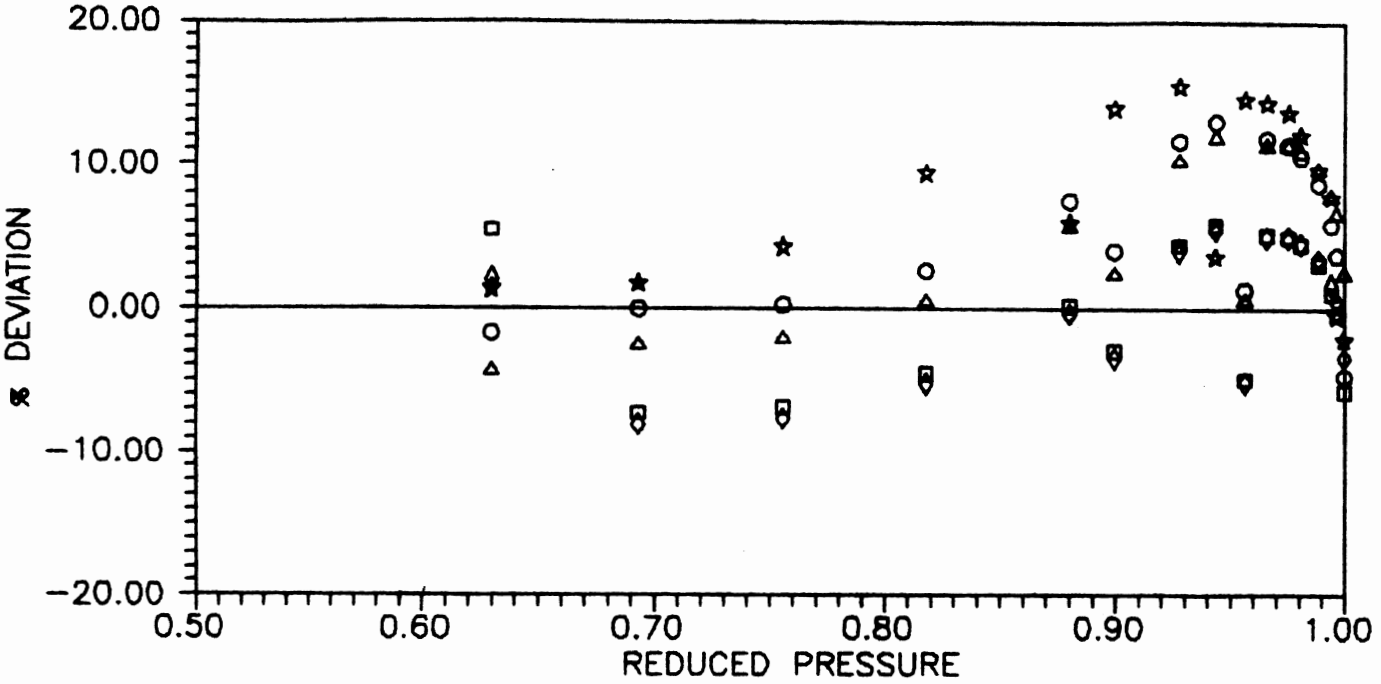

Figure 18b. Saturated Vapor Density Predictions for CO_2 + Benzene at 344.3 K Using PR EOS with Scaled-Volume Translation

documented better error distributions for the scaled-volume translation in comparison with those for original PR EOS and Peneloux's VT predictions given in Figures 17a and 17b.

CHAPTER IV

SCALED-VARIABLE-REDUCED-COORDINATE APPROACH

The Scaled-Variable-Reduced-Coordinate (SVRC) method has been developed for the prediction of pure-fluid properties in the saturation region. In this condition, only one fluid property is required to fix the state of the system. According to this approach saturated properties may be related to the independent correlating variable as:

$$Y = \{Y_c^{\alpha} - (Y_c^{\alpha} - Y_t^{\alpha})\theta\}^{(1/\alpha)} \tag{38}$$

where Y is a saturated fluid property and θ is a correlation function of ε which is related to the independent variable by the following expression:

$$\varepsilon = \frac{X_c - X}{X_c - X_t} \tag{39}$$

Mixture Liquid Density Model

The SVRC liquid density model developed by Shaver [30] for pure fluids is extended to mixtures. Using this model, the extension task involves determination of the functions θ and α of Equation (38) for a mixture. The original

definitions for θ and α were employed in this study, where

$$\theta = \frac{1 - A^{\varepsilon^{B}}}{1 - A} \tag{40}$$

and α given by the relation

$$\frac{\alpha_c - \alpha}{\alpha_c - \alpha_t} = \frac{1 - A^{\varepsilon}}{1 - A} \tag{41}$$

For an isothermal binary mixture, ε is defined as:

$$\varepsilon = \frac{P_c - P}{P_c - P_i} \tag{42}$$

where P_i = the lowest pressure in the isotherm

A = correlation constant

B = theoretical scaling-law exponent value of 0.325

α_c = the limiting value of α at the critical point

α_t = the limiting value of α at the lowest pressure

When dealing with mixtures, one may evaluate α_c and α_t or $\Delta\alpha$ (= $\alpha_c - \alpha_t$) by fixing the model parameters with existing mixture data, or by using values of α_c and $\Delta\alpha$ obtained from pure-fluid data applied to mixtures by employing appropriate mixing rules.

The values of any mixture property obtained from a model are sensitive to the mixing rules applied. Therefore, an evaluation of the existing mixing rules and the relevant theories become a necessity before they may be applied for

the SVRC approach. Appendix C contains a brief discussion on this topic.

The generalized equations for α_c and $\Delta\alpha$ used for pure fluids have been presented by Shaver [30] as:

$$\Delta\alpha_i = C_1 + C_2 T_{rt_i}^{(C_3 + C_4 Z_{c_i})} \tag{43}$$

and

$$\alpha_{c_i} = C_5 + C_6 T_{rt_i}^{(C_7 + C_8 \omega_i)} \tag{44}$$

where T_{rt} is triple point temperature and subscript i represents component i. Values for the constants A and B in Equation (40) and C_1 through C_8 in Equation (43) and (44) are listed in Table XII.

For a given mixture, once θ, α, and ε are determined, liquid density can be calculated according to Equation (38):

$$\rho = \{\rho_c^{\alpha} - (\rho_c^{\alpha} - \rho_i^{\alpha})\ \theta\ \}^{(1/\alpha)} \tag{45}$$

where ρ_i is the lowest density in the isotherm and ρ_c is the critical value.

Mixture Vapor Density Model

Following Shaver [30], forms of θ and α similar to those used for liquid density were chosen for the correlation of vapor density,

TABLE XII

GENERALIZED LIQUID DENSITY CORRELATION PARAMETERS [30]

Parameter	Value
A	1.07068
B	0.325
C_1	3.63493
C_2	-3.73713
C_3	0.32786
C_4	-0.90951
C_5	0.36141
C_6	2.95802
C_7	16.4993
C_8	-25.4640

$$\theta = \frac{2 - A_1^{\varepsilon\, B_1} - A_2^{\varepsilon\, B_2}}{2 - A_1 - A_2} \tag{46}$$

and

$$\frac{\alpha_c - \alpha}{\alpha_c - \alpha_t} = \frac{2 - A_1^{\varepsilon\, c} - A_2^{\varepsilon}}{2 - A_1 - A_2} \tag{47}$$

where α_c and $\Delta\alpha$ for component i are estimated using the following relation:

$$\alpha_{c_i} = C_1 T_{rt_i}^{C_2} + C_3 Z_{c_i}^{C_4} + [C_3^{(Z_{c_i} - 0.29)} + C_5^{\omega_i} + C_6^{(3\omega_i - \omega_i/Z_{c_i})} - 3\,] \tag{48}$$

and

$$\Delta\alpha_i = C_1 T_{rt_i}^{C_2} + C_3 Z_{c_i}^{C_4} + (C_1 - 1)\, T_{rt_i}^{C_4} + [C_3^{(Z_{c_i} - 0.29)} - 1.0]\, C_7 \tag{49}$$

Values for the constants A_1, A_2, B_1, B_2, C, and C_1 through C_7 are listed in Table XIII. The definition for ε and the calculation procedure for vapor density are the same as those for the liquid density model.

A variety of cases were evaluated in the course of this work, as documented in Table XIV. The results for every case are presented in Tables XV through Table XIX.

In Case 10, all the model parameters were regressed in order to investigate the model precision in representing

TABLE XIII

GENERALIZED VAPOR DENSITY CORRELATION PARAMETERS [30]

Parameter	Values
A_1	3.110
A_2	0.600
B_1	0.325
B_2	1.325
C	0.600
C_1	0.2998
C_2	0.4365
C_3	0.9884
C_4	0.8631
C_5	0.7532
C_6	0.9489
C_7	30.704

TABLE XIV

DESCRIPTION OF CASES USED TO EVALUATE THE SVRC METHOD

Case	Description
10	A, α_c, $\Delta\alpha$, ρ_i and ρ_c are regressed for liquid A_1, A_2, α_c, $\Delta\alpha$, ρ_i and ρ_c are regressed for vapor. In Case A: P_i and ρ_i in Equations (44) and (45) are defined as the saturated pressure and saturated density of HC at the corresponding temperature. In Case B: P_i and ρ_i in Equations (44) and (45) are defined as the lowest pressure and the lowest density of the available experimental data.
11	A and α_c are generalized; P_i and ρ_i are defined as in Case 10.
12	α_c and $\Delta\alpha$ are evaluated according to the following mixing rules: $\alpha_c = (\Sigma_i (z_i \alpha_{c_i})^m)^{1/m}$ and $\Delta\alpha = (\Sigma z_i \Delta\alpha_i)$ P_i and ρ_i are defined as in Case 10, and m is regressed separately for liquid and vapor.

TABLE XIV (Continued)

Case	Description
13	Mixing rules applied are the same as in Case 12, P_i and ρ_i are defined as in Case 10, and m is generalized.
14	Mixing rules applied are the same as in Case 12, P_i and ρ_i are defined as in Case 10, and A and m are generalized.

existing experimental data. In this case ρ_i and ρ_c were also treated as regressed parameters. Excellent fit was achieved, where 0.42 % AAD and 0.81 % AAD were obtained for saturated liquid and vapor density predictions, respectively (including pure fluid densities, Case A). However, possible errors in the pure fluid density data may be inferred from Table XV, where the predictions without pure fluid densities (Case B) gave markedly better results (0.18 and 0.38 % AAD for liquid and vapor, respectively).

Generalization of the SVRC model using two parameters (A and α_c) in Case 11 gives good representation for liquid density predictions (1.99 and 1.39 % AAD for Case A and Case B, respectively). By comparison, vapor density predictions gave mediocre results.

An alternative method to extending the SVRC model to mixtures was pursued through a set of mixing rules. Cases 12-14 present the mixing rules employed in this study. These rules are an extension of the conformal solution mixing rules described in Appendix C. By contrast, this method of calculating phase densities, where pure component α_c and $\Delta\alpha$ are used, is less precise than that presented by Cases 10-11. As indicated by Tables XVII-XIX, the quality of the density predictions (about 3 % AAD for both liquid and vapor densities for Case 12) suggest the need for more refinement in estimating the mixture model parameters.

Effect of the independent variable (pressure) on the model is shown in Figure 19 for the CO_2 + benzene system.

TABLE XV

SATURATED DENSITY PREDICTIONS USING SVRC[a]
Case 10: ALL PARAMETERS REGRESSED

Mixture CO_2 +	No Pts	T, K	Case A % AAD		Case B % AAD	
			Liquid	Vapor	Liquid	Vapor
n-Butane	22	319.26	1.26	1.61	0.63	0.83
	16	344.26	0.36	0.61	0.20	0.32
	16	377.59	0.12	0.47	0.08	0.22
n-Decane	22	344.26	0.77	0.51	0.22	0.47
	25	377.59	0.26	0.37	0.05	0.23
n-Tetra-decane	21	344.26	0.42	0.76	0.13	0.22
Benzene	17	344.26	0.18	0.26	0.16	0.16
c-Hexane	15	344.26	0.26	0.24	0.16	0.38
t-Decalin	33	344.26	0.09	1.69	0.01	0.47
Overall Statistics:			0.42	0.81	0.18	0.38

Case A: including pure fluid densities

Case B: excluding pure fluid densities

a. A, α_c, $\Delta\alpha$, ρ_i and ρ_c are regressed for liquid

A_1, A_2, α_c, $\Delta\alpha$, ρ_i and ρ_c are regressed for vapor

TABLE XVI

SATURATED DENSITY PREDICTIONS USING SVRC
Case 11: A & α_c GENERALIZED

Mixture CO_2 +	No Pts	T, K	Case A % AAD		Case B % AAD	
			Liquid	Vapor	Liquid	Vapor
n-Butane	22	319.26	3.52	6.89	3.68	1.56
	16	344.26	1.18	4.23	0.83	1.55
	16	377.59	3.23	2.16	1.24	1.12
n-Decane	22	344.26	2.66	1.94	1.32	1.23
	25	377.59	1.05	7.67	1.31	0.94
n-Tetra-decane	21	344.26	2.94	12.42	0.32	5.00
Benzene	17	344.26	0.97	7.28	0.08	7.75
c-Hexane	15	344.26	1.08	6.19	0.64	5.77
t-Decalin	33	344.26	1.31	9.61	1.67	7.64
Overall Statistics:			1.99	6.84	1.39	3.76
Parameters A:			0.0100	5.1182	0.0108	9.8753
α_c:			-8.6313	0.6973	-6.7871	0.0011

Case A: including pure fluid densities

Case B: excluding pure fluid densities

TABLE XVII

SATURATED DENSITY PREDICTIONS
USING SVRC WITH MIXING RULES
Case 12: m REGRESSED

Mixture CO_2 +	No Pts	T, K	Case A % AAD		Case B % AAD	
			Liquid	Vapor	Liquid	Vapor
n-Butane	22	319.26	4.68	1.56	3.25	1.82
	16	344.26	2.40	0.80	1.63	0.39
	16	377.59	1.15	0.54	0.91	0.59
n-Decane	22	344.26	5.62	3.61	2.69	0.53
	25	377.59	3.55	1.51	0.53	0.35
n-Tetra-decane	21	344.26	3.87	3.53	1.79	0.94
Benzene	17	344.26	2.20	1.69	0.95	0.26
c-Hexane	15	344.26	2.34	2.11	1.03	0.57
t-Decalin	33	344.26	1.74	4.52	0.41	2.75
Overall Statistics:			3.13	2.43	1.44	1.07

Case A: including pure fluid densities

Case B: excluding pure fluid densities

TABLE XVIII

SATURATED DENSITY PREDICTIONS
USING SVRC WITH MIXING RULES
Case 13: m GENERALIZED

Mixture CO_2 +	No Pts	T, K	Case A % AAD		Case B % AAD	
			Liquid	Vapor	Liquid	Vapor
n-Butane	22	319.26	5.87	12.41	4.61	3.91
	16	344.26	2.40	10.08	1.62	1.78
	16	377.59	2.97	5.83	1.80	1.17
n-Decane	22	344.26	5.66	17.87	3.19	5.91
	25	377.59	3.55	16.30	0.65	5.80
n-Tetra-Decane	21	344.26	3.87	21.76	1.79	10.87
Benzene	17	344.26	2.87	4.37	2.76	1.59
C-Hexane	15	344.26	2.91	2.63	1.02	0.63
t-Decalin	33	344.26	1.87	15.60	0.73	12.37
Overall Statistics:			3.56	12.86	1.97	5.78
Parameter m:			0.1833	0.4138	0.2007	0.4516

Case A: including pure fluid densities

Case B: excluding pure fluid densities

TABLE XIX

SATURATED DENSITY PREDICTIONS
USING SVRC WITH MIXING RULES
Case 14: A & m GENERALIZED

Mixture CO_2 +	No Pts	T, K	Case A % AAD		Case B % AAD	
			Liquid	Vapor	Liquid	Vapor
n-Butane	22	319.26	4.08	8.40	3.88	2.86
	16	344.26	1.87	4.90	1.28	1.03
	16	377.59	3.38	3.86	1.46	1.57
n-Decane	21	344.26	3.99	3.69	2.46	1.91
	25	377.59	1.75	7.87	0.40	0.75
n-Tetra-decane	21	344.26	3.33	11.43	1.10	6.49
Benzene	17	344.26	2.59	7.38	2.48	6.53
c-Hexane	15	344.26	1.80	5.78	1.02	4.75
t-Decalin	33	344.26	0.33	9.48	0.47	8.42
Overall Statistics:			2.47	7.30	1.56	4.08
Parameters	A:		0.0469	100.00	0.1476	5.6332
	m:		-0.0451	1.5272	-0.3926	1.8078

Case A : including pure fluid densities

Case B : excluding pure fluid densities

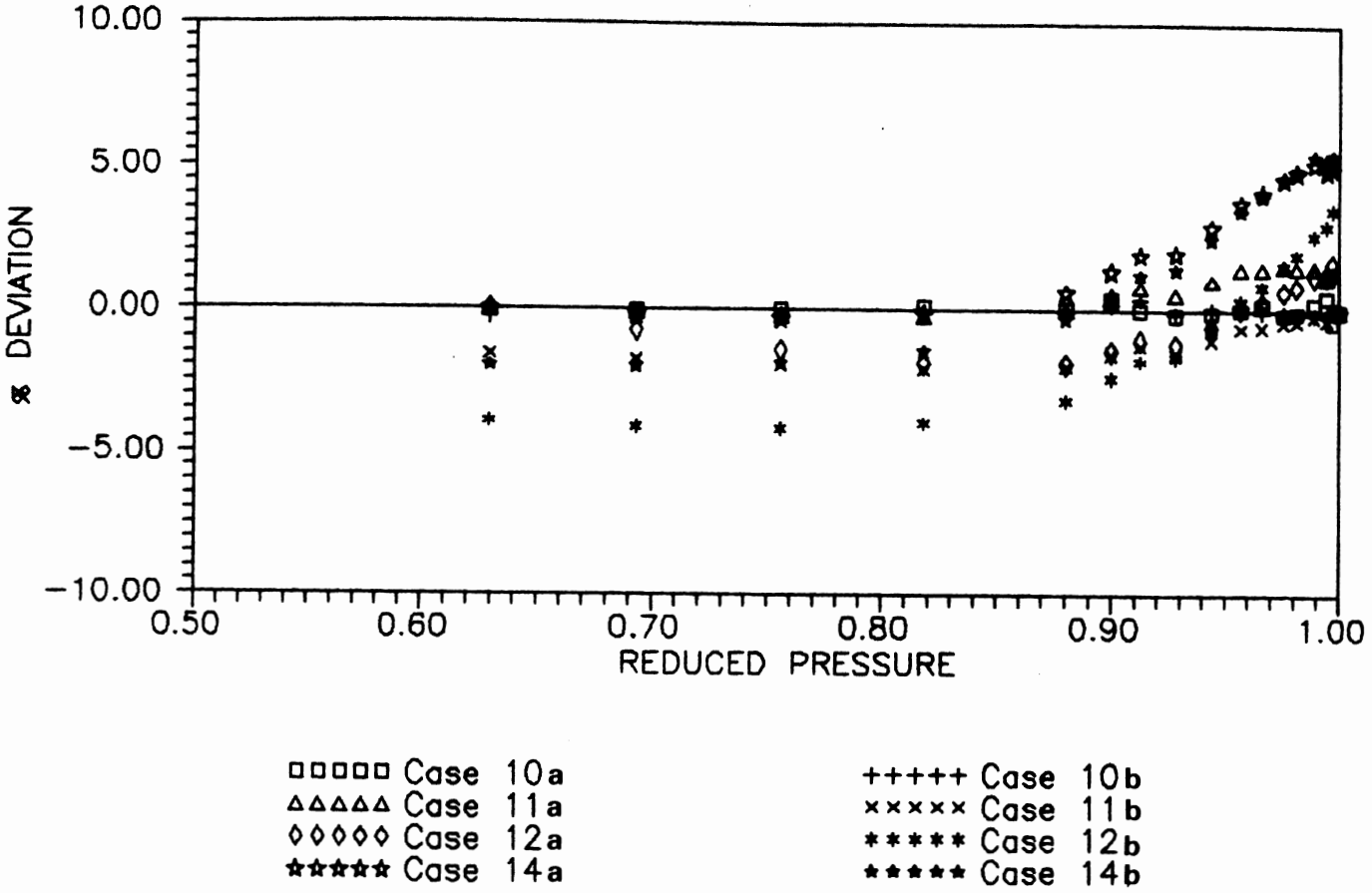

Figure 19a. Saturated Liquid Density Predictions for CO_2 + Benzene at 344.3 K Using SVRC

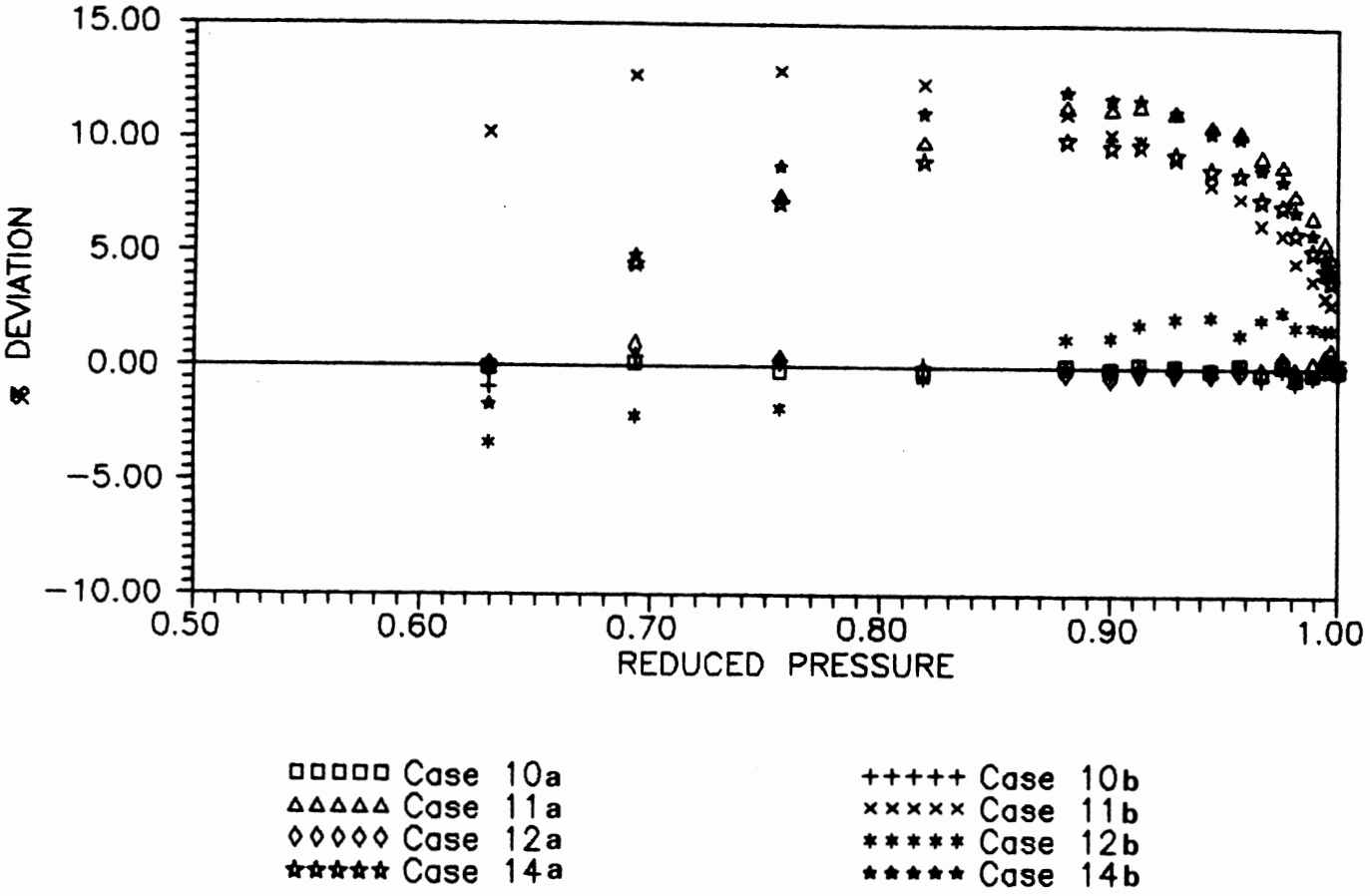

Figure 19b. Saturated Vapor Density Predictions for CO_2 + Benzene at 344.3 K Using SVRC

In general, all the cases evaluated using the SVRC method show similar error distribution. More significantly, the relative deviation tends to be small near the critical point.

CHAPTER V

COMPARISON OF DENSITY PREDICTION MODELS

As shown in the previous chapter, in general, the PR EOS gives better results when compared with the other two cubic equations of state (RK and SRK). Therefore, the PR EOS was used to evaluate the volume translation models studied, and only the PR EOS is used in the comparison to follow for the density prediction models.

Table XX presents a summary of the results for the density models considered in this study. To assess the abilities of the proposed models for phase density predictions, two equally important aspects of model development are considered. First, the models' abilities to precisely represent the existing experimental data through regressed model parameters as represented by model evaluation cases. Second, the predictive capability of the generalized-parameter models.

As reported in Table XX and illustrated by Figure 20, the scaled-volume translation gives significantly better results than those obtained for the PR EOS fitted with two interaction parameters. While, in general, comparable predictions are obtained from Peneloux's volume translation, improved representation of the near-critical density

TABLE XX

SUMMARY OF RESULTS FOR MODEL EVALUATION AND PARAMETER GENERALIZATION

Case	Models	% AAD	
		Liquid	Vapor
----------	Model Evaluation	----------	
2	PR, regressed C_{ij}	3.39	3.16
3	PR, regressed C_{ij} and D_{ij}	1.37	2.24
5a	PR with Peneloux VT	4.79	6.20
5b	PR with Peneloux VT	1.67	2.54
7a	PR with Scaled-VT	4.96	4.71
7b	PR with Scaled-VT	0.66	2.71
8a	PR with Scaled-VT	5.31	6.66
8b	PR with Scaled-VT	2.08	5.71
10a	SVRC, including pure fluid densities	0.42	0.81
10b	SVRC, exluding pure fluid densities	0.18	0.38
12a	SVRC, mixing rules regressed m	3.13	2.43
12b	SVRC, mixing rules regressed A and m	1.44	1.07
----------	Parameter Generalizations	----------	
1	PR, $C_{ij} = 0$, $D_{ij} = 0$	6.35	13.52
6	PR with Peneloux VT	4.57	7.63
9	PR with Scaled-VT	6.24	10.19
11a	SVRC, including pure fluid densities	1.99	6.84
11b	SVRC, exluding pure fluid densities	1.39	3.76
13a	SVRC, mixing rules	3.56	12.86
13b	SVRC, mixing rules	1.97	5.78
14a	SVRC, mixing rules	2.47	7.30
14b	SVRC, mixing rules	1.56	4.08

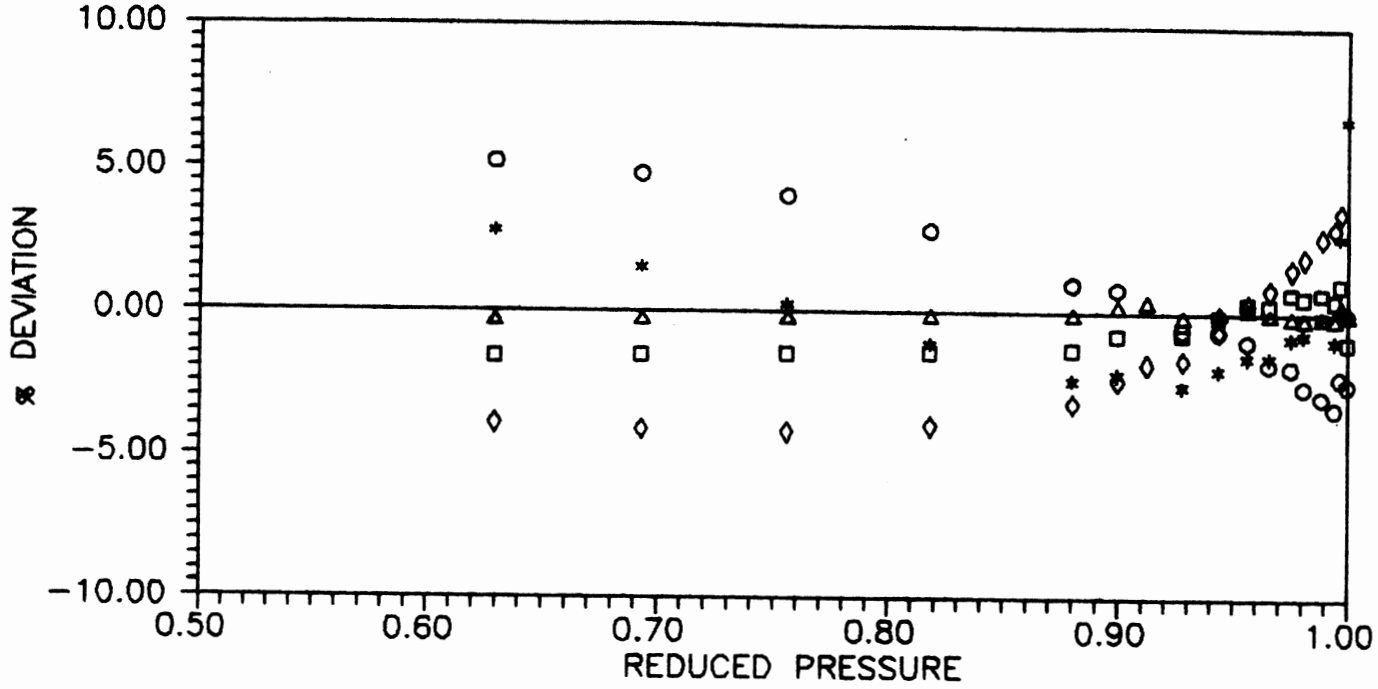

ooooo PR EOS
***** Peneloux
□□□□□ This work : Case 8a
ΔΔΔΔΔ This work : Case 10
◊◊◊◊◊ This work : Case 12

Figure 20a. Saturated Liquid Density Predictions for CO2 + Benzene at 344.3 K: Model Evaluation Cases

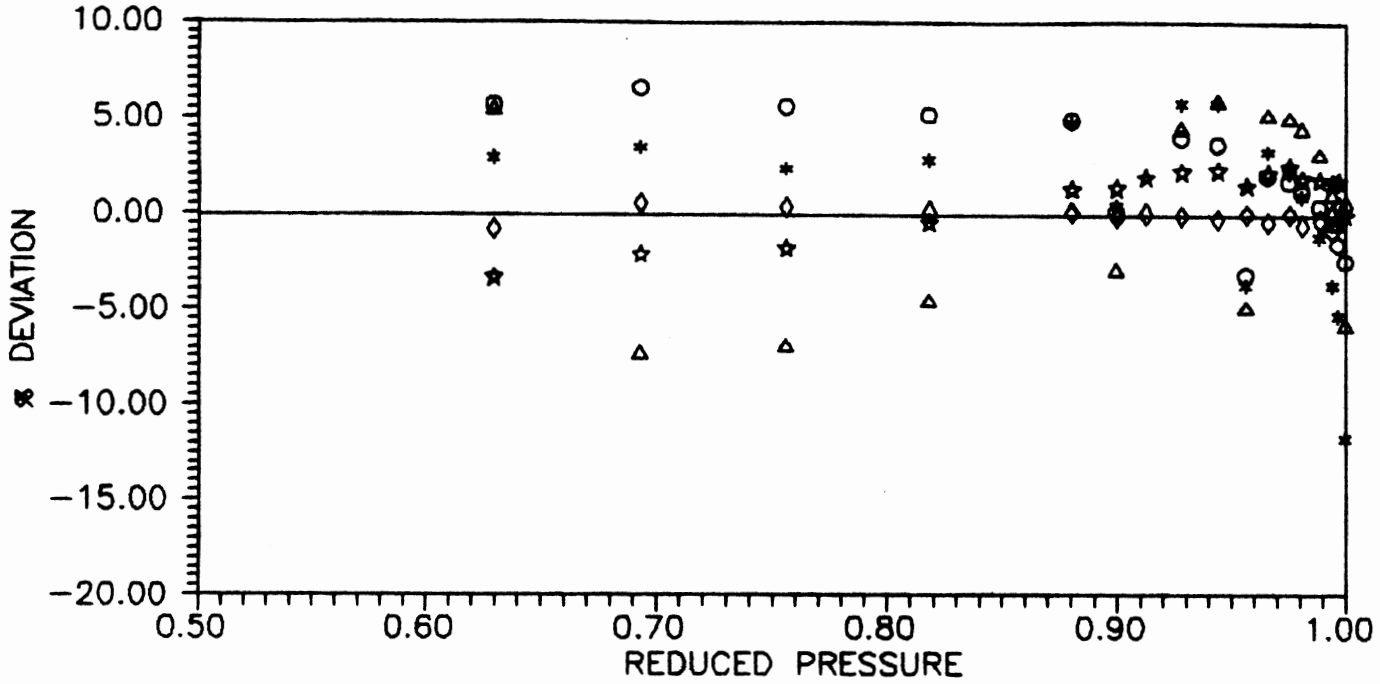

ooooo PR EOS
***** Peneloux
ΔΔΔΔΔ This work : Case 8a
◊◊◊◊◊ This work : Case 10
★★★★★ This work : Case 12

Figure 20b. Saturated Vapor Density Predictions for CO2 + Benzene at 344.3 K: Model Evaluation Cases

predictions favors the scaled-volume translations.

EOS methods aside, the available comparisons reveal excellent correlation capabilities for the SVRC model, as indicated by Cases 10 (AAD within 0.5 %) and 12 of Table XX. Similarly Figure 20 documents that both the overall quality of the fit and the error distribution for the SVRC model are superior to those obtained for the EOS methods.

For the systems considered in this study, the quality of the density predictions for the liquid phase is consistently better than that obtained for the vapor phase. Moreover, separate treatment of liquid and vapor in both the translation models and the SVRC model gives better results than regressing the model parameters simultaneously using liquid and vapor density data.

Figure 21 addresses comparisons of the generalized-parameter predictions, as exemplified by CO2 + Benzene binary. For liquid densities, deviations from the various models reveal similar trends to those observed in model evaluation using regressed parameters. As expected, the original PR EOS gives poor near-critical density predictions (up to 25 % AAD). While Peneloux's volume translation improves predictions far from the critical, little improvements are realized by this method near the critical point.

In comparison, the scaled-volume translation succeeds in improving the quality of the near-critical region, but fails to affect significant improvements overall. These

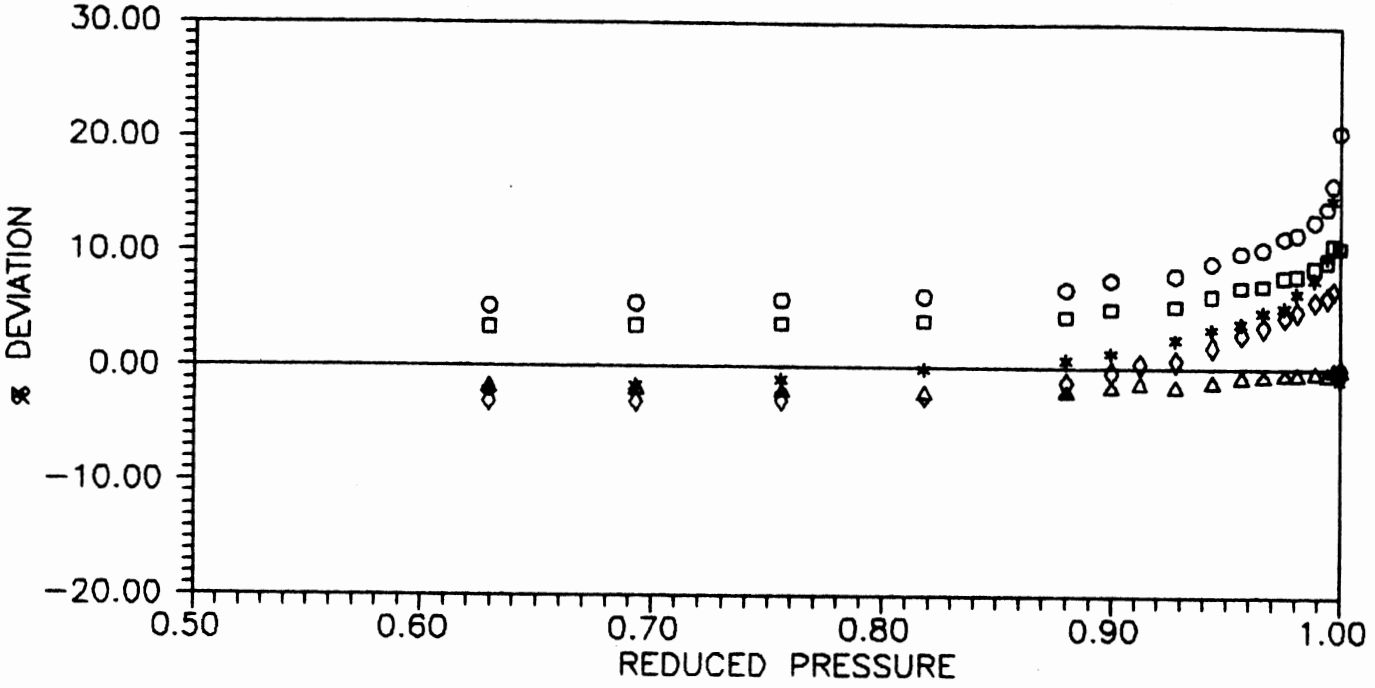

ooooo Original PR
***** Peneloux
□□□□□ This work : Case 9
ΔΔΔΔΔ This work : Case 11
◊◊◊◊◊ This work : Case 14

Figure 21a. Saturated Liquid Density Predictions for CO2 + Benzene at 344.3 K: Model Generalization Cases

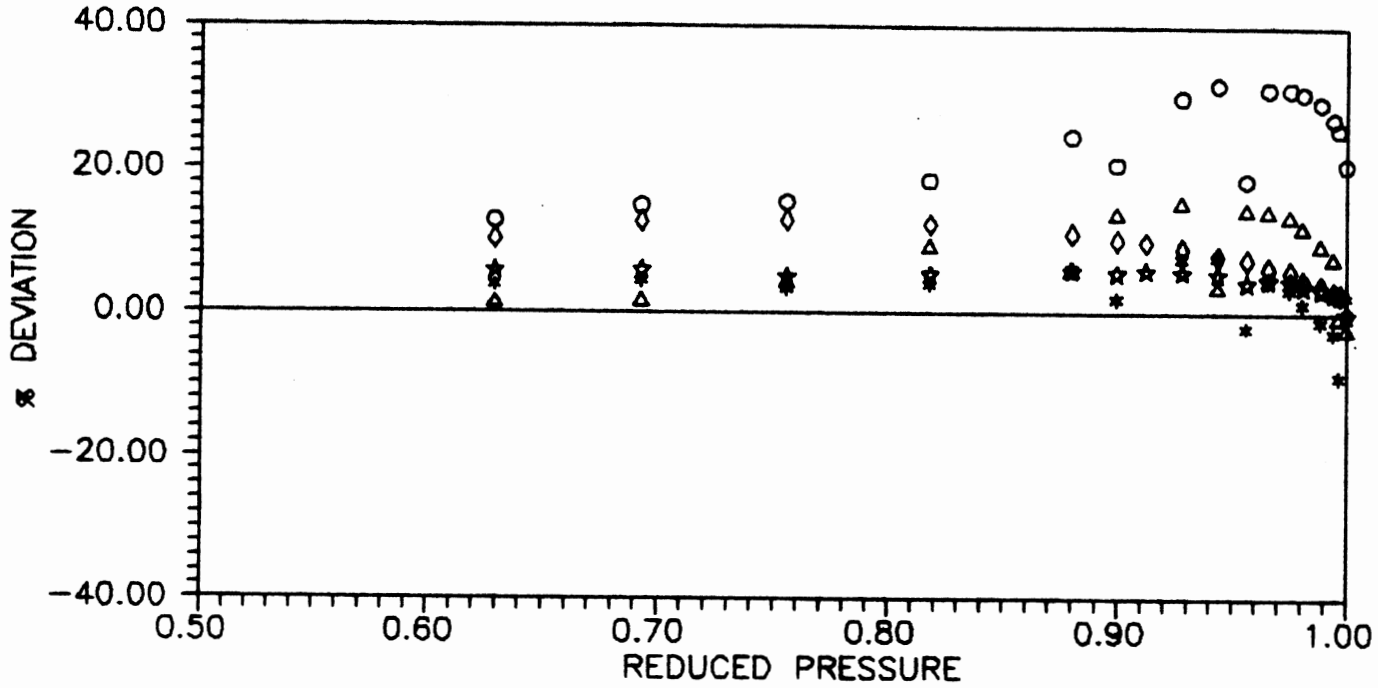

ooooo Original PR
***** Peneloux
ΔΔΔΔΔ This work : Case 9
◊◊◊◊◊ This work : Case 11
★★★★★ This work : Case 14

Figure 21b. Saturated Vapor Density Predictions for CO2 + Benzene at 344.3 K: Model Generalization Cases

results indicate a deficiency in the proposed parameter generalizations, and the need for further development to realize the full potential of this translation procedure.

Good results are realized using the generalized SVRC model. Overall deviations of 2 % AAD for the liquid density predictions (Case 11), including predictions near the critical point, support this assessment. As indicated by the results of Case 14, the proposed mixing rules do not enhance the vapor density predictions, i.e., accounting for the effects of composition in the generalized parameters is inconsequential.

For vapor densities, the proposed generalized predictions produce minor improvement over the original PR EOS (Case 1). Perhaps, the only exception to this trend is the better SVRC predictions, including the near critical region as shown in Figure 21. This assessment confirms the conclusion reached earlier that a better strategy for parameter generalization is required.

Clearly, while the generalized predictions exhibit marked deterioration in the quality of the density predictions, they represent the rationale vehicle for an a priori predictive capability.

In summary, the proposed models compare favorably with existing literature correlations with the added advantages of (a) covering the full saturation range up to the critical point of the mixture and (b) the inherent simplicity. The model parameter generalizations demonstrate a potential for

a reasonably accurate predictive capability, especially for liquid densities. Additional work, however, is required to achieve this objective.

CHAPTER VI

CONCLUSIONS AND RECOMMENDATIONS

The functional behavior of van der Waals type cubic equations of state have been evaluated. As part of this evaluation, the reduced form of the equation of state, F(Z), and its derivatives have been mapped for selected pure fluids and mixtures. The results, which have involved several test systems, suggest an effective strategy for the solution of cubic EOS.

To improve EOS phase density predictions, a new volume translation method has been developed. While the new method compares favorably with Peneloux's volume translation procedure, it has the added advantage of accounting for scaling-law behavior near the critical point. Experimental phase density measurements for a number of CO2/hydrocarbon binaries were employed in our evaluations. The quality of the density predictions, using regressed parameters, is reasonable as indicated by a 0.7 and 2.7 % AAD fit for the liquid and vapor, respectively. In comparison, the generalized-parameter predictions using this method do not constitute a significant improvement over the existing procedures and will require further refinement.

Parallel to our evaluations of EOS density predictions,

corresponding states methods have been considered. Specifically, the scaled-variable-reduced-coordinate approach was extended to the prediction of mixture phase densities. Utility of this approach is demonstrated by correlation of isothermal saturated liquid and vapor densities of CO2 + hydrocarbon mixtures at pressures from the vapor pressure of the hydrocarbon solvent to the critical point of the mixture. This new correlation results in excellent representation of saturated liquid densities (0.42 % AAD) and saturated vapor densities (0.82 % AAD) of the mixtures.

Generalized SVRC correlations provide adequate liquid and vapor density predictions (2 and 7 %AAD, respectively). The quality of these predictions, however, is enhanced by the flexibility offered by one system-specific parameter. Further, simplicity of the SVRC model combined with its clear advantage in covering the full saturation range in accordance with scaling-law behavior near the critical region, suggest an expanded investigation to realize the full potential of the model.

Additional data for mixture phase densities, involving a variety of chemical species, are required for a thorough assessment of the proposed methods to improve density predictions.

LITERATURE CITED

1. ASHRAE Handbook & Product Directory 1977 Fundamentals. New York: ASHRAE Inc.; 1977.

2. Abbot, M. M. Cubic equation of state. AIChE Journal 19(3):596-601; 1973.

3. Asseleneau, L.; Bocdanic, G.; Vidal, J. A versatile algorithm for calculating vapour-liquid equilibria. Fluid Phase Equilibria 3:273-290; 1979.

4. Benedek, P.; Olti, F. Computer aided chemical thermodynamics of gases and liquids. New York: John Wiley & Sons; 1985.

5. Campbell, S. W. A good initial estimate for pure component vapour pressure in equation of state calculation. Industrial Engineering Chemistry - Research 27:1333-1335; 1988.

6. Charoensombut-Amon, T.; Martin, R. J.; Kobayashi, R. Application of generalized multi property apparatus to measure phase equilibrium and vapor phase densities of supercritical carbon dioxide in n-hexadecane systems up to 26 MPa. Fluid Phase Equilibria 31:89-104; 1986.

7. Chou, G. F.; Prausnitz, J. M. A phenomenological correction to an equation of state for the critical region. AIChE Journal 35:1485-1496; 1989.

8. Constantinides, A. Applied numerical methods with personal computer. New York: McGraw Hill; 1988.

9. Dulcamara, Jr., P. B. Interfacial tensions for carbon dioxide or light hydrocarbons in hydrocarbon solvents: Experimental data and correlations. Stillwater: Oklahoma State University; 1986. Masters Thesis.

10. Edmister, C. W.; Lee, B. I. Applied hydrocarbon thermodynamics. Houston, TX: Gulf Publishing Co.; 1984.

11. Firoozabadi, A.; Nutakki, R.; Wong, T. W.; Aziz, K. EOS predictions of compressibility and phase behavior in systems containing water, hydrocarbons, and CO_2. SPE Reservoir Engineering. 1988 May:673.

12. Gasem, K. A. M. Binary vapor-liquid equilibrium for carbon dioxide + heavy normal paraffins. Stillwater: Oklahoma State University; 1986. Ph. D. Dissertation.

13. Gasem, K. A. M.; Dickson, K. B.; Dulcamara, P. B.; Nagarajan, N.; Robinson, Jr., R. L. Equilibrium phase compositions, phase densities, and interfacial tensions for CO_2 + hydrocarbon systems. 5. CO_2 + n-tetradecane. Journal of Chemical Engineering Data 34:191-195; 1989.

14. Gasem, K. A. M. Chemical engineering thermodynamics. Class notes. Stillwater: Oklahoma State University; 1991.

15. Gosset, R.; Heyen, G.; Kalitventzeff, B. An efficient algorithm to solve cubic equation of state. Fluid Phase Equilibria 25:51-64; 1985.

16. Hankinson, R. W.; Thomson, G. H. A new correlation for saturated densities of liquids and their mixtures. AIChE Journal 24(4):653-662; 1979.

17. Jovanovic, S.; Paunivic, R.; Mihajlov, A. An efficient method to avoid trivial solutions in bubble point pressure calculations from a cubic equation of state. Proceedings of the 3rd Austrian-Italian-Yugoslav Chemical Engineering Conference. 1982 Sept. Vol I:80.

18. Kay, W. B. Density of hydrocarbon gases and vapor. Industrial and Engineering Chemistry 28:1014-1019; 1936.

19. Mansoori, A. G. Mixing rules for cubic equations of state. In: Chao, K. C.; Robinson, Jr., R. L., ed. Equation of state: theories and applications. Washington, D. C.: American Chemical Society; 1986:314-330.

20. Martin, J. J. Cubic equations of state - Which ?. Industrial Engineering Chemistry - Fundamental 18(2): 81-97; 1979.

21. Michelsen, M. L. Calculation of phase envelopes and critical points for multicomponent mixtures. Fluid Phase Equilibria 4:1-10; 1980.

22. Michelsen, M. L. The isothermal flash problem part I, Stability. Fluid Phase Equilibria 9:1-19; 1982.

23. Michelsen, M. L. The isothermal flash problem part II, phase-split calculation. Fluid Phase Equilibria 9:21-40; 1982.

24. Nagarajan, N.; Robinson, Jr., R. L. Equilibrium phase compositions, phase densities, and interfacial tensions for CO_2 + hydrocarbon systems. 2. CO_2 + n-decane. Journal of Chemical Engineering Data 31:168-171; 1986.

25. Peneloux, A.; Rauzy, E. A consistent correction for Redlich-Kwong-Soave volumes. Fluid Phase Equilibria 8:7-23; 1982.

26. Poling, B. E.; Grens II, E. A.; Prausnitz, J. M. Thermodynamic properties from a cubic equation of state: Avoiding trivial roots and spurious derivatives. Industrial Engineering Chemistry - Process 20:127-130; 1981.

27. Prausnitz, J. M.; Lichtenthaler, R. N.; Gomes de Azevedo E. Molecular thermodynamics of fluid phase equilibria. Inglewood Cliffs, NJ: Prentice Hall Inc.; 1986.

28. Sandler, S. I. From molecular theory to thermodynamic models. Chemical Engineering Education; 1990:12.

29. Sengers, J. V; Levelt Sengers, J. M. H. A universal representation of thermodynamic properties of fluids in the critical region. International Journal of Thermophysics 5(2):195-209; 1984.

30. Shaver, R. D. A new scaled variable reduced coordinate, framework for correlation of pure fluid saturation properties. Stillwater: Oklahoma State University; 1990. Masters Thesis.

31. Spencer, C. F.; Danner, R. P. Prediction of bubble-point density of mixtures. Journal of Chemical Engineering Data 18:230-236; 1973.

32. Stryjek, R.; Vera, J. H. PRSV2: A cubic equation of state for accurate vapor-liquid equilibria calculations. The Canadian Journal of Chemical Engineering 64:820-826; 1986.

33. Tung Tsang; Hammarstrom, C. A. A consistent rule for selecting roots in cubic equations of state. Industrial Engineering Chemistry 26:857-859; 1987.

34. Turek E. A.; Metcalfe, R. S.; Yarborough, L.; Robinson, Jr., R. L. Phase Equilibria in CO_2 - multicomponent hydrocarbon systems: Experimental data and an improved prediction technique. Society of Petroleum Engineers Journal. 1984 June:308-323.

35. Van Ness, H. C.; Abbot, M. M. Classical thermodynamics of nonelectrolyte solutions. New York: McGraw-Hill; 1982.

36. Vargaftik, N.B. Tables on the thermophysical properties of liquids and gases. New York: John Wiley & Sons Inc.; 1975.

37. Veeranna, D.; Rihani, D. N. Avoiding convergence problems in VLE predictions using an equation of state. Fluid Phase Equilibria 16:41-45; 1984.

38. Vidal, J. Equations of state - reworking the old forms. Fluid Phase Equilibria 13:15-33; 1983.

39. Wegner, F. J. Corrections to scaling laws. Physical Review B, 5:4529-4536; 1972.

40. Yen, L. C.; Woods, S. S. A generalized equation for computer calculation of liquid densities. AIChE Journal 12:95-99; 1966.

41. Yu J.-M.; Adachi, Y.; Lu, B. C.-Y. Selection and design of cubic equation of state. In: Chao, K. C.; Robinson, Jr., R. L., ed. Equation of state: theories and applications. Washington, D. C.: American Chemical Society; 1986:537-559.

APPENDIX A

DATABASE EMPLOYED

TABLE A.1

PURE COMPONENT PHYSICAL PROPERTIES USED

Name	MW	T_t, K	T_c, K	P_c, Bar	ω	Z_c	Source
CO_2	44.01	216.58	304.21	73.8254	0.2251	0.2756	36
n-Butane	319.26	134.86	425.16	37.9614	0.2004	0.2754	36
n-Decane	344.26	243.5	617.55	20.9672	0.4885	0.2481	36
n-Tetra-decane	344.26	267.0	692.95	15.7307	0.6442	0.2258	36
Benzene	344.26	278.68	562.16	48.9805	0.2120	0.2714	36
c-Hexane	344.26	279.7	553.5	40.7002	0.2120	0.2724	36
t-Decalin	344.26	*	681.5	29.4653	0.2860	0.2132	**

* not available, an estimate was used.

** Gasem, K. A. M., Private communication, Oklahoma State University, Stillwater, OK, 1991.

TABLE A.2

SOURCE AND RANGES OF SATURATED DENSITY DATA FOR THE MIXTURES

Mixture CO_2 +	T, K	Pressure Range, Bar	Liquid Density Range, Kg/m^3	Vapor Density Range, Kg/m^3	Source
n-Butane	319.26	21.79 - 76.26	563.4 - 406.0	50.1 - 406.0	42
	344.26	32.06 - 81.22	520.1 - 373.5	69.1 - 373.5	
	377.59	28.82 - 75.70	456.5 - 319.5	71.4 - 319.5	
n-Decane	344.26	63.85 - 127.41	708.1 - 590.5	130.3 - 590.5	24
	377.59	103.42 - 164.85	676.0 - 553.5	205.1 - 553.5	
n-Tetra-decane	344.26	110.32 - 163.82	750.8 - 708.5	296.1 - 708.5	13
Benzene	344.26	68.95 - 109.56	815.0 - 533.0	156.0 - 533.0	43
c-Hexane	344.26	68.74 - 109.63	734.8 - 525.0	149.3 - 525.0	43
t-Decalin	344.26	103.42 - 158.37	834.3 - 765.8	270.9 - 765.8	*

42. Hsu, Jack J. C.; Nagarajan, N.; Robinson, Jr., R. L. Journal of Chemical Engineering Data 30:485; 1985.

43. Nagarajan, N.; Robinson, Jr., R. L. Journal of Chemical Engineering Data 30:485; 1985.

* Gasem, K. A. M. Private communication, Oklahoma State University, Stillwater, OK, 1991.

TABLE A.3

SATURATION PROPERTIES OF PURE HYDROCARBONS

Hydro-carbon	T, K	Pressure, Bar	Liquid Density, Kg/m^3	Vapor Density, Kg/m^3	Source
n-Butane	319.26	4.48	549.7	11.1	1,36
	344.26	8.34	515.2	20.7	
	377.59	16.66	460.1	43.7	
n-Decane	344.26	0.07	688.7	0.6	24,36
	377.59	0.14	663.2	1.0	
n-Tetra-decane	344.26	0.07	724.3	3.4	36
Benzene	344.26	0.76	821.5	4.0	36
c-Hexane	344.26	0.76	727.8	3.3	36
t-Decalin	344.26	0.07	828.8	4.6	*

* Gasem, K. A. M., Private communication, Oklahoma State University, Stillwater, OK, 1991.

APPENDIX B

CORRELATION PARAMETERS

This appendix presents the correlation parameters for the various cases considered. In all our model evaluations, the following objective function was employed:

$$S = \Sigma \left(\frac{\rho_{exp} - \rho_{calc}}{\rho_{calc}} \right)^2$$

A Marquart non-linear regression procedure was used in the calculations.

TABLE B.1

CUBIC EOS PARAMETERS

Mixture CO_2 +	EOS	Case 2	Case 3	
		C_{ij}	C_{ij}	D_{ij}
n-Butane	RK	0.088644	0.230051	-0.188969
	SRK	0.082032	0.186184	-0.141123
	PR	0.104740	0.139597	-0.043457
n-Decane	RK	-0.153113	0.328671	-0.335056
	SRK	-0.156333	0.125041	-0.194337
	PR	0.013626	0.135960	-0.089068
n-Tetra-decane	RK	-0.404795	0.273381	-0.379790
	SRK	-0.316447	0.099021	-0.253351
	PR	-0.078937	0.159804	-0.153784
Benzene	RK	0.163156	0.370428	-0.267122
	SRK	0.112182	0.250898	-0.174424
	PR	0.169880	0.216535	-0.058558
c-Hexane	RK	0.173305	0.376230	-0.247319
	SRK	0.127108	0.260001	-0.158654
	PR	0.186487	0.219611	-0.039096
t-Decalin	RK	-0.000304	0.374319	-0.288048
	SRK	-0.045614	0.231245	-0.206361
	PR	0.125471	0.222058	-0.076084

TABLE B.2

PENELOUX'S VOLUME TRANSLATION PARAMETERS a_1 AND a_2 REGRESSED SIMULTANEOUSLY (CASE 5a)

Mixture CO_2 +	a_1	a_2
n-Butane	0.470524	0.209416
n-Decane	0.788640	0.261139
n-Tetra-decane	0.399181	0.266551
Benzene	23.2463	0.272606
c-Hexane	29.0035	0.273077
t-Decalin	0.534079	0.232791

TABLE B.3

PENELOUX'S VOLUME TRANSLATION PARAMETERS
a_1 AND a_2 REGRESSED SEPARATELY
(CASE 5b)

Mixture CO_2 +	T, K	Liquid		Vapor	
		a_1	a_2	a_1	a_2
n-Butane	319.26	0.362084	0.234275	0.266215	-0.18874
	344.26	0.086888	0.125744	0.223235	-0.11494
	377.59	0.080528	0.204327	0.198155	-0.06393
n-Decane	344.26	0.273552	0.271674	1.81010	0.26490
	377.59	0.566088	0.263372	0.994246	0.26179
n-Tetra-decane	344.26	0.182235	0.296528	1.84333	0.26505
Benzene	344.26	10.1989	0.272136	0.217670	-0.02853
c-Hexane	344.26	9.91893	0.272410	0.199653	-0.06834
t-Decalin	344.26	0.192789	0.230347	3.02291	0.25316

TABLE B.4

SCALED-VOLUME TRANSLATION PARAMETERS
A_1 AND A_2 REGRESSED SIMULTANEOUSLY
(CASE 7a)

Mixture CO_2 +	T, K	A_1	A_2
n-Butane	319.26	1.42506	0.691348
	344.26	1.23367	0.786342
	377.59	1.29379	0.772529
n-Decane	344.26	1.03345	0.977117
	377.59	1.01029	0.995004
n-Tetra-decane	344.26	0.967254	1.04456
Benzene	344.26	0.912547	0.961514
c-Hexane	344.26	0.967271	0.925745
t-Decalin	344.26	0.816206	1.09705

TABLE B.5

SCALED-VOLUME TRANSLATION PARAMETERS
A_1 AND A_2 REGRESSED SEPARATELY
(CASE 7b)

Mixture CO_2 +	T, K	Liquid		Vapor	
		A_1	A_2	A_1	A_2
n-Butane	319.26	1.09968	0.871935	1.71517	0.586171
	344.26	1.10570	0.881794	1.33410	0.721654
	377.59	1.19703	0.852493	1.36584	0.716951
n-Decane	344.26	0.97488	0.992446	1.10580	0.958755
	377.59	1.04773	0.990162	0.977639	0.999124
n-Tetra-decane	344.26	1.06350	1.00912	0.862806	1.09300
Benzene	344.26	0.994632	0.948988	0.820323	0.986490
c-Hexane	344.26	1.00482	0.941191	0.936149	0.913551
t-Decalin	344.26	1.04761	0.968863	0.677259	1.20157

TABLE B.6

SCALED-VOLUME TRANSLATION PARAMETERS
A_1 REGRESSED SEPARATELY

Mixture CO_2 +	T, K	Case 8a	Case 8b	
			Liquid	Vapor
		A_1	A_1	A_1
n-Butane	319.26	0.822335	0.900484	0.764259
	344.26	0.861240	0.917671	0.816233
	377.59	0.909486	0.963478	0.865728
n-Decane	344.26	0.996273	0.963271	1.03433
	377.59	1.00053	1.02774	0.975987
n-Tetra-decane	344.26	1.03942	1.07939	1.00079
Benzene	344.26	0.849205	0.904928	0.799828
c-Hexane	344.26	0.847781	0.906101	0.801964
t-Decalin	344.26	0.953062	0.993123	0.918655

TABLE B.7

SVRC PARAMETERS FOR LIQUID DENSITY PREDICTIONS

Mixture CO_2 +	T, K	Case 10a			Case 12a m
		A	α_c	$\Delta\alpha$	
n-Butane	319.26	0.026267	-3.25615	-15.2007	0.062500
	344.26	0.067437	-2.12181	-14.6838	0.180712
	377.59	0.435370	0.77178	-7.4440	0.222790
n-Decane	344.26	0.026495	-0.20533	-49.3740	0.062500
	377.59	0.018398	-4.93761	-18.9649	0.075390
n-Tetra-decane	344.26	0.001000	0.75115	-0.8579	0.062500
Benzene	344.26	0.23182	0.19349	-17.5439	0.197354
c-Hexane	344.26	0.02802	-3.10072	-15.6389	0.172738
t-Decalin	344.26	0.30867	-10.5752	-30.5783	0.062500

TABLE B.8

SVRC PARAMETERS FOR LIQUID DENSITY PREDICTIONS

Mixture CO_2 +	T, K	Case 10b			Case 12b
		A	α_c	$\Delta\alpha$	m
n-Butane	319.26	0.001000	-15.2650	-19.5733	0.155428
	344.26	0.069781	0.00028	-3.56684	0.196818
	377.59	0.375540	-0.06962	-15.1311	0.231330
n-Decane	344.26	0.001000	-17.0399	-28.7716	0.084479
	377.59	0.049022	4.31625	-47.0878	0.192956
n-Tetra-decane	344.26	0.001000	0.02743	-19.4467	0.062500
Benzene	344.26	0.320030	0.00412	-9.15922	0.242570
c-Hexane	344.26	0.216594	0.00397	-17.3546	0.198799
t-Decalin	344.26	0.064313	-0.31274	-3.49246	0.164696

TABLE B.9

SVRC PARAMETERS FOR VAPOR
DENSITY PREDICTIONS

Mixture CO_2 +	T, K	Case 10a				Case 12a
		A_1	A_2	α_c	$\Delta\alpha$	m
n-Butane	319.26	2.02318	0.781285	1.01215	0.00311	0.482230
	344.26	3.10577	0.742682	0.80706	0.00142	0.490771
	377.59	3.03170	0.923471	0.84293	-0.01421	0.467343
n-Decane	344.26	100.000	1.67133	0.37096	-0.41720	0.300971
	377.59	6.02836	1.23487	0.73311	0.00558	0.299926
n-Tetra-decane	344.26	100.000	7.04806	0.61102	1.21592	0.257173
Benzene	344.26	2.08445	0.55941	1.47354	0.45818	0.439815
c-Hexane	344.26	2.33096	0.37165	1.70828	1.33356	0.425453
t-Decalin	344.26	100.000	5.18088	0.47535	0.48836	0.311244

TABLE B.10

SVRC PARAMETERS FOR VAPOR DENSITY PREDICTIONS

Mixture CO_2 +	T, K	Case 10b				Case 12b m
		A_1	A_2	α_c	$\Delta\alpha$	
n-Butane	319.26	2.24160	0.492084	1.68107	0.93668	0.513196
	344.26	7.06976	1.24805	0.01862	-0.34811	0.484681
	377.59	2.83805	1.00604	0.82369	0.12693	0.471044
n-Decane	344.26	6.86321	1.28410	0.34999	-0.00399	0.309281
	377.59	5.23001	1.41423	0.32774	0.05951	0.279335
n-Tetra-decane	344.26	1.37160	1.27609	2.98049	2.23821	0.197302
Benzene	344.26	2.25373	0.66949	1.31288	0.51754	0.518940
c-Hexane	344.26	2.70774	0.69533	0.82182	0.11106	0.457936
t-Decalin	344.26	1.75915	2.96031	0.65934	1.76050	0.248796

APPENDIX C

MIXING RULES

Evaluation of the mixture molar properties may be achieved through three different ways. One may use mixing rules which employ the pure molar properties at the mixture conditions, use the mixing rules within the EOS parameters, or use mixing rules applied to the critical properties, as typically done when using CST methods.

For an ideal solution, the molar volume of a mixture is often calculated by summing up the pure molar volumes at the same conditions:

$$V = \sum_{i}^{N} x_i \, V_i \qquad (C.1)$$

However, this simple relation cannot be applied for real fluids. The partial property concept offers a formal definition for mixture property in terms of constituent contributions [14]:

$$V = \sum_{i}^{N} x_i \, \tilde{V}_i \qquad (C.2)$$

In which $\tilde{V}_i$ is partial molar volume of "i" in solution, defined by

$$\tilde{V}_i = \left(\frac{\partial V}{\partial n_i} \right)_{n_j, T, P} \qquad (C.3)$$

Furthermore, the deviation function concept allows us to calculate mixture properties in terms of their deviation from a selected model, see, e.g., [14]:

$$X^D = X - X^{model} \tag{C.4}$$

Applying Equation (C.4) for volume and by choosing an ideal solution as the selected model, we obtain

$$\Delta V^m = V - V^{id}$$

or

$$V = \Delta V^m + V^{id} = \Delta V^m + \sum_i^N x_i V_i \tag{C.5}$$

One may evaluate V or ΔV^m using corresponding states method or EOS method.

Corresponding States Theory

The principle of corresponding states asserts that physical properties are dependent on intermolecular forces. This may be expressed as a function of compressibility factor as [27]:

$$Z = Z\left(\frac{\varepsilon}{kT}, \frac{V}{N\sigma^3}\right) \tag{C.6}$$

in which:

ε = energy parameter of molecular interaction

σ = molecular separation corresponding to the minimum potential energy of interaction

k = Boltzmann's constant

Further, it has been shown that Equation (C.6) may be expressed in terms of reduced temperature, reduced specific volume and as many substance dependent parameter as necessary:

$$Z = Z\ (T_r,\ V_r,\ a_1,\ a_2,\ .....\ a_n\ ) \qquad (C.7)$$

The saturated liquid and vapor densities can also be related to the temperature as:

$$V = V\ (T_r,\ a_1,\ a_2,\ .....a_n) \qquad (C.8)$$

When the liquid is pure, it is clear that ε and σ in Equation (C.6) are potential parameters for that pure liquid. These parameters can be determined from second virial coefficients, transport properties, critical data, etc. When the liquid is a mixture, however, ε and σ depend on the mole fraction in some manner about which corresponding states theory itself tells us little.

Extension of the corresponding states theory to mixtures suggested a theory called *one-fluid theory* [27]. This theory is based on the fundamental idea that a mixture can be considered to be a hypothetical pure fluid whose characteristic molecular size and energy are those of the mixture components. In macroscopic terms, the effective critical properties (pseudicritical) of the mixture are composition averages of the component critical properties. These might be written in the following formulation [26]:

$$\varepsilon_m = f_\varepsilon\ (x_1,\ \varepsilon_1,\ \varepsilon_2) \qquad (C.9)$$

$$\sigma_m = f_\sigma\ (x_1,\ \sigma_1,\ \sigma_2) \qquad (C.10)$$

$$T_{cm} = f_{T_c}\ (x_1,\ T_{c1},\ T_{c2}) \qquad (C.11)$$

$$P_{cm} = f_{P_c}(x_1, P_{c1}, P_{c2}) \tag{C.12}$$

$$V_{cm} = f_{V_c}(x_1, V_{c1}, V_{c2}) \tag{C.13}$$

for a binary system.

The first practical application of this idea was made by Kay (1936) when he suggested to find the gas-phase compressibility factor of a mixture of hydrocarbons from a generalized compressibility factor diagram based on volumetric data for pure hydrocarbon gases. Kay used a particularly simple mixing rules for relating the reducing parameters for a mixture to the composition. More realistic mixing rules have been proposed by various authors [16,31,35].

In accordance with this one-fluid theory, Equation (C.8) can also be extended for the mixtures. A good example is given by the model developed by Rackett and modified by Spencer and Danner in 1972 [31]. They proposed the following correlation to predict pure liquid density.

$$V = (RT_c/P_c)\ ZRA^{[1+(1-T_r)^{2/7}]} \tag{C.14}$$

and for liquid mixtures:

$$V = V_{cm}\ ZRA_m^{(1-T/T_{cm})^{2/7}} \tag{C.15}$$

Where ZRA is the Rackett compressibility factor. V_{cm} is obtained by blending pure-component critical volumes

(Kay's rule) and T_{cm} is obtained using the following mixing rules:

$$T_{cm} = \Sigma\ \Phi_i\ T_{ci} \tag{C.16}$$

where

$$\Phi_i = \frac{x_i\ V_{ci}}{\Sigma\ x_i\ V_{ci}} \tag{C.17}$$

Another example is one proposed by Hankinson and Thomson in 1979 [16]:

$$(Vs/V^o) = Vr^{(o)}\ [1 - \omega_{SRK}\ Vr^{(d)}] \tag{C.18}$$

The suggested mixing rules are:

A. $$T_{cm} = \frac{\Sigma_i \Sigma_j\ x_i x_j\ V_{ij}^o\ T_{cij}}{V_m^o} \tag{C.19}$$

$$V_m^o = 1/4\ \{\ \Sigma\ x_i V_i^o + 3(\ \Sigma\ x_i V_i^{o\ 2/3})\ (\Sigma\ x_i V_i^{o\ 1/3})\} \tag{C.20}$$

$$V_{ij}^o\ Tc_{ij} = (V_i^o\ T_{ci}\ V_j^o\ T_{cj}\ )^{1/2} \tag{C.21}$$

B. $$T_{cm} = \Sigma\ x_i\ V_i^o\ T_{ci}\ /\ \Sigma\ x_i\ V_i^o \tag{C.22}$$

V_m^o is given by Equation (C.20)

C. $$T_{cm} = [\Sigma\ x_i\ V_i^o\ (T_{ci})^{1/2}]^2\ /\ (\Sigma\ x_i V_i^o)^2 \tag{C.23}$$

The acentric factor was estimated in two ways:

$$\omega_m = \Sigma\ x_i \omega_{SRKi} \tag{C.24}$$

or

$$\omega_m = \frac{\Sigma\, x_i V_i^o\, \omega_{SRKi}}{x_i V_i^o} \qquad (C.25)$$

EOS Method

Application of equations of state to mixtures is generally achieved by introduction of mixing rules in the EOS parameters. Appropriate mixing rules may be derived from the conformal solution theory (see, e.g., Mansoori [19]).

The conformal solution mixing rules may be written in general as:

$$f = f\,(f_{ij},\, h_{ij},\, x_i) \qquad (C.26)$$

and

$$h = h\,(f_{ij},\, h_{ij},\, x_i) \qquad (C.27)$$

f and h are the molecular conformal volume parameter and the molecular conformal energy parameter, respectively. Functional forms of these mixing rules cannot be derived from any general theory but depend on particular assumptions which one chooses to make about the structure of the solution. Therefore different theories of mixtures will result in different mixing rules.

Mansoori derived several of these functional forms from the Statistical Mechanical Theory using two different mixture theory approximations; one-fluid theory and multi-fluid theory. However several assumptions were still needed in order to simplify the mixing rules. As an example, by using Conformal Solution Approximation (CSA) for

one-fluid theory, one will obtain the following mixing rule:

$$f\,h = \sum_{i}^{N}\sum_{j}^{N} x_i\, x_j\, f_{ij}\, h_{ij} \qquad (C.28)$$

and

$$h = \sum_{i}^{N}\sum_{j}^{N} x_i\, x_j\, h_{ij} \qquad (C.29)$$

Other functional forms derived from other theories of mixtures can be found in Mansoori's article [19].

In the formulation of a mixture theory, the combining rules for unlike-interaction potential parameters are also needed. These may be expressed as follows:

$$f_{ij} = (1-C_{ij})(f_{ii}\, f_{jj})^{1/2} \qquad (C.30)$$

and

$$h_{ij} = (1+D_{ij})\,[(h_{ii}^{1/3} + h_{jj}^{1/3})/2\,]^3 \qquad (C.31)$$

In which C_{ij} and D_{ij} are adjustable parameters.

In order to apply the conformal solution mixing rules for cubic equation of state, we should notice that parameter b of cubic EOS is proportional to molecular volume, or $b \propto h$, and parameter a is proportional to molecular volume times molecular energy, or $a \propto f\,h$. Therefore Equations (C.28), (C.29), (C.30) and (C.31) become:

$$a = \sum_{i}^{N}\sum_{j}^{N} x_i\, x_j\, a_{ij} \qquad (C.32)$$

$$b = \sum_{i}^{N}\sum_{j}^{N} x_i\, x_j\, b_{ij} \qquad (C.33)$$

$$a_{ij} = (1-C_{ij})\ b_{ij}\ (a_{ii}\ a_{jj}/b_{ii}\ b_{jj})^{1/2} \qquad (C.34)$$

and

$$b_{ij} = (1+D_{ij})\ [(b_{ii}^{1/3} + b_{jj}^{1/3})/2]^3 \qquad (C.35)$$

If we adopt a geometric-mean combination rules [35]:

$$a_{ij} = (a_{ii}\ a_{jj})^{1/2} \qquad (C.36)$$

and

$$b_{ij} = (b_{ii}\ b_{jj})^{1/2} \qquad (C.37)$$

Equation (C.32) and (C.33) become:

$$a = (\Sigma\ x_i\ a_i^{1/2})^2 \qquad (C.38)$$

and

$$b = (\Sigma\ x_i\ b_i^{1/2})^2 \qquad (C.39)$$

The power 1/2 in the combination rules can be replaced by constants 1/m for Equation (C.36) and 1/n for Equation (C.37). When we do so, the following mixing rules are suggested:

$$a = (\Sigma\ (x_i\ a_i)^{1/m})^m \qquad (C.39)$$

and

$$b = (\Sigma\ (x_i\ b_i)^{1/n})^n \qquad (C.40)$$

VITA

Mahmud Sudibandriyo

Candidate for the Degree of

Master of Science

Thesis: IMPROVED METHODS FOR PHASE DENSITY PREDICTION: CO_2 + HYDROCARBONS

Major Field: Chemical Engineering

Biographical:

Personal Data: Born in Pati, Indonesia, August 18, 1963, the son of H. Mohammad Oelwi and Siti Kamari.

Education: Graduated from SMPP X Yogyakarta, Indonesia, in June 1981; received Bachelor of Engineering Degree in Chemical Engineering from Bandung Institute of Technology, Indonesia, in June 1986; completed requirements for the Master of Science Degree at Oklahoma State University in May, 1991.

Professional Experience: Junior Lecturer, Gas and Petrochemical Department, University of Indonesia, from 1986 - present.